CHARACTERIZATION AND BIOFABRICATION OF KERATINOCYTES AT THE SINGLE-CELL LEVEL IN NORMAL AND PATHOLOGICAL CONDITIONS

A Thesis Submitted to
the Graduate School of Engineering and Sciences of
İzmir Institute of Technology
in Partial Fulfillment of the Requirements for the Degree of

MASTER OF SCIENCE

in Bioengineering

by
Alara KARA

July 2024
İZMİR

We approve the thesis of **Alara KARA**

Examining Committee Members:

_____

Prof. Dr. Engin ÖZÇİVİCİ
Department of Bioengineering, İzmir
Institute of Technology

_____

Prof. Dr. Özden Yalçın Özuysal
Department of Bioengineering, İzmir
Institute of Technology

_____

Asst. Prof. Dr. Yavuz Oktay
Department of Medical Biology, Dokuz
Eylül University

12 July 2024

_____

Prof. Dr. Engin ÖZÇİVİCİ
Supervisor, Department of
Bioengineering

_____   _____

Assoc. Prof. Dr.Ceyda ÖKSEL   **Prof. Dr. Mehtap EANES**
Head of the Department of   Dean of the Graduate School of
Bioengineering   Engineering and Sciences

ACKNOWLEDMENTS

ABSTRACT

CHARACTERIZATION AND BIOFABRICATION OF KERATINOCYTES AT THE SINGLE-CELL LEVEL IN NORMAL AND PATHOLOGICAL CONDITIONS

Keratinocytes are crucial for skin protection thus overall health. They are often modeled in cell culture studies to promote structural integrity and wound healing purposes. This study aims to develop precise methods using magnetic levitation technique for measuring keratinocyte density at the single cell level and to investigate how variations in measurements affect keratinocyte behavior and function in normal and pathological conditions. In addition, through MagLev technology, we seek to create 3D keratinocyte constructs and assess their structural integrity and functionality for tissue engineering. In this study four different HaCaT cell groups were used to examine their behavior in a magnetic field.

Our single cell density measurements revealed significant differences, particularly in the G45E group, demonstrating standardization and reproducibility for HaCaT cells. Previous studies have determined the density of various cell types, but keratinocytes were examined for the first time in this context.

In biofabrication experiments, significant levitation height differences were noted in the G45E group, further confirming our experimental standardization. Magnetic levitation culture transferred to agarose resulted in more consistent spheroid structures compared to direct transfer, which formed disorganized structures. Thus, keratinocyte structures maintained their integrity with magnetic levitation, facilitating further 3D culture.

The results improve the understanding of the biophysical properties of keratinocytes and demonstrate that label-free, scaffold-free magnetic levitation can be a practical alternative for tissue engineering. This approach via negative magnetophoresis offers significant potential in bioengineering at the cell and tissue level to create complex 3D structures without conventional scaffolds, providing a novel, density-based detection method.

ÖZET

NORMAL VE PATOLOJİK KOŞULLARDA KERATİNOSİTLERİN TEK HÜCRE DÜZEYİNDE KARAKTERİZASYONU VE BİYOFABRİKASYONU

Keratinositler cildin korunması ve dolayısıyla genel sağlık için çok önemlidir. Yapısal bütünlüğü ve yara iyileşmesini desteklemek amacıyla hücre kültürü çalışmalarında sıklıkla modellenmektedirler. Bu çalışma, keratinosit yoğunluğunu tek hücre düzeyinde ölçmek için manyetik kaldırma tekniğini kullanarak hassas yöntemler geliştirmeyi ve ölçümlerdeki varyasyonların normal ve patolojik koşullarda keratinosit davranışını ve işlevini nasıl etkilediğini araştırmayı amaçlamaktadır. Buna ek olarak, MagLev teknolojisi aracılığıyla 3D keratinosit yapıları oluşturmayı ve bunların doku mühendisliği için yapısal bütünlüğünü ve işlevselliğinin değerlendirilmesi amaçlanmaktadır. Bu çalışmada, manyetik alandaki davranışlarını incelemek için dört farklı HaCaT hücre grubu kullanılmıştır.

Tek hücre yoğunluğu ölçümlerimiz, özellikle G45E grubunda HaCaT hücreleri için standardizasyon ve tekrarlanabilirliği gösteren önemli farklılıklar ortaya koymuştur. Önceki çalışmalarda çeşitli hücre tiplerinin yoğunluğu belirlenmiştir, ancak keratinositler bu bağlamda ilk kez incelenmiştir.

Biyofabrikasyon deneylerinde, G45E grubunda deneysel standardizasyonumuzu daha da doğrulayan önemli levitasyon yüksekliği farklılıkları kaydedilmiştir. Agaroza aktarılan manyetik levitasyon kültürü, dağınık yapılar oluşturan doğrudan aktarıma kıyasla daha tutarlı sferoid yapılarla sonuçlanmıştır. Böylece, keratinosit yapıları manyetik kaldırma ile bütünlüklerini korumuş ve daha fazla 3D kültürü oluşumunu kolaylaştırmıştır.

Sonuçlar keratinositlerin biyofiziksel özelliklerinin anlaşılmasını geliştirmekte ve etiketsiz, iskelesiz manyetik kaldırmanın doku mühendisliği için pratik bir alternatif olabileceğini göstermektedir. Bu yaklaşım negatif manyetoforez yoluyla, geleneksel iskeleler olmadan karmaşık 3D yapılar oluşturmak için hücre ve doku düzeyinde biyomühendislik çalışmalarına önemli bir potansiyel sunmakta ve yeni, yoğunluğa dayalı bir tespit yöntemi sağlamaktadır.

TABLE OF CONTENTS

LIST OF FIGURES

LIST OF TABLES

CHAPTER 1

INTRODUCTION

1.1. Magnetic Levitation Basic Principles

Magnetic levitation methodology uses a magnetic field gradient to manipulate objects remotely. This principle is applied to various scientific and technological applications, including biotechnology (Karakuzu et al., 2024; Sarigil et al., 2019).

There are two main techniques of magnetic levitation: positive magnetophoresis and negative magnetophoresis. Positive magnetophoresis involves labeling cells with magnetic beads, causing them to move to regions of higher magnetic field and enabling the separation of magnetic and non-magnetic samples (Dabbagh et al. 2021; Torres-Cruz et al. 2023). This technique has been used for separating different cell types, such as blood cells, lipid cells and cancer cells, and for 3D cell culture (Anil-Inevi et al. 2021; Durmus et al. 2015; Sarigil et al. 2019; Yaman et al., 2018; Zhu et al. 2014). However, positive magnetophoresis technique requires additional cell labeling steps that is not only time-consuming, but also potentially cytotoxic for the cells of interest.

Negative magnetophoresis on the other hand, is a label-free technique that can induce a weightlessness environment (Hu, Krishaa, and Fong 2023; Yaman et al. 2018). Basic principle of negative magnetophoresis depend on the weak repulsion of diamagnetic objects under strong magnetic fields. Diamagnetic substances, including water, minerals, proteins, DNA, and most cell types, acquire a net magnetic moment opposite to the magnetic field when placed within it, due to the rearrangement of their electron's spin and orbital motions (Munaz, Shiddiky, and Nguyen 2018; Yaman et al., 2018). This magnetic moment causes objects to be slightly repelled by external magnetic fields. A simple way to increase the response of diamagnetic substances to an applied magnetic field is to immerse diamagnetic objects in paramagnetic liquids, which have a

larger magnetic susceptibility than diamagnetic substances (Yang et al. 2016). The attraction of paramagnetic liquids by the magnetic field causes diamagnetic substances to act as magnetic holes and move to regions with a weaker magnetic field (Yaman et al., 2018; Yamato and Kimura 2020). This technique has been used for density measurement, cell separation (Durmus et al., 2015; Sarigil et al., 2019) (Figure 1), cell sorting (Kecili et al. 2023) (Figure 2), and 3D biofabrication (Anil-Inevi et al., 2021), making it a versatile tool for biotechnology applications (Ashkarran and Mahmoudi 2021; Baday et al. 2015)

.
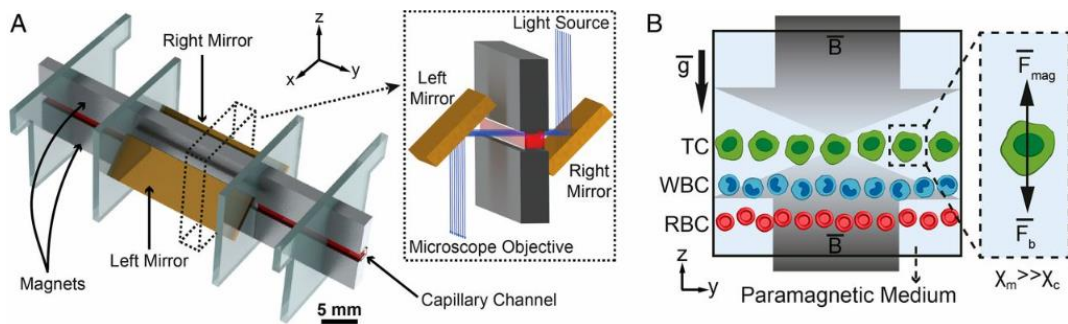
Figure 1. Operating mechanism of the magnetic levitation device: Principles of the MagDense cell density meter. (A) Diagram of the device setup (B) Equilibrium heights of various cells (Tumor Cells, White Blood Cells, Red Blood Cells) during magnetic levitation. Due to magnetic induction (B) and gravitational forces (g), cells are levitated within the channel and settle at an equilibrium plane where magnetic forces balance them (Source: Durmus et al., 2015).

For cell detection applications, magnetic levitation enables label-free detection and separation of cells based on small single cell density differences, allowing a precise manipulation of cells for high-resolution imaging and analysis, and facilitating the observation of cell behavior in a levitated, 3D environment mimicking in vivo conditions (Lyu et al., 2024; Turnbull et al. 2020; Zhao et al. 2016). In biofabrication, magnetic levitation assists in forming intricate 3D tissue structures by precisely controlling cell placement, enhances tissue engineering by allowing cells to self-assemble into desired patterns and improves the fabrication of tissue constructs with consistent distribution and strong structural integrity (Figure 3) (Anil-Inevi et al. 2021a; Parfenov et al. 2020).
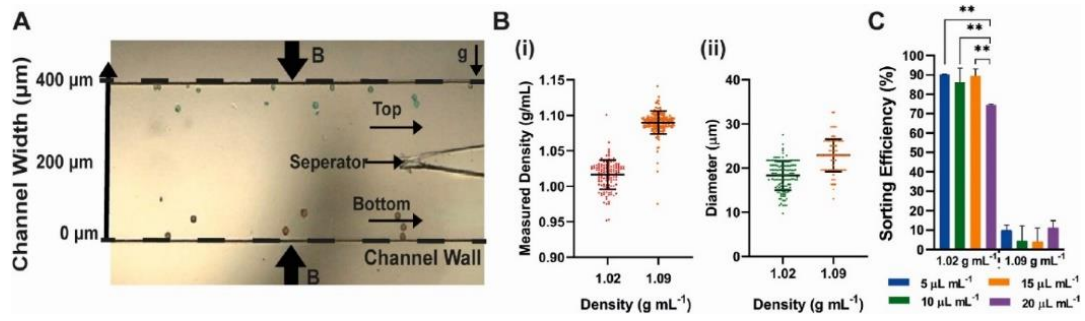
Figure 2. Magnetic levitation sorting device: (A) High (red) and Low (Green) density beads in the microfluidic channel with a separator under magnetic field (B) Measured density and diameter of beads (C) Sorting efficiency of beads (Source: Kecili et al. 2023).
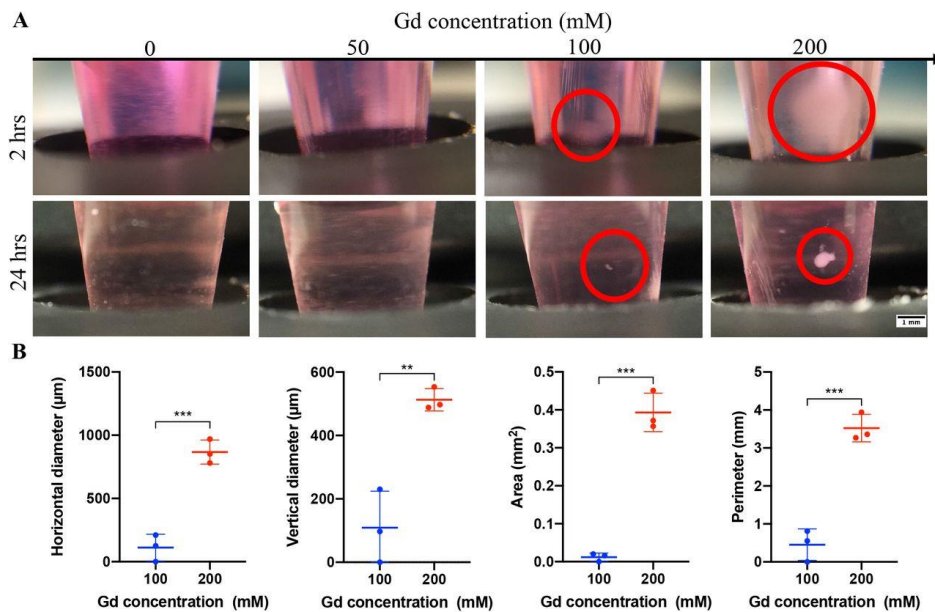
Figure 3. Self-assembly of mesenchymal stem cells in magnetic levitation system. (A) Short term (2 hrs) or 24 hrs of culture photographs of D1 ORL UVA cells in different Gd3+ concentrations. Scale bar: 1 mm. (B) Size analysis of the cellular clusters formed for 24 hrs with magnetic levitation **: $p < 0.01$; ***: $p < 0.001$. (Source: Anil-Inevi et al. 2021a).

Magnetic levitation (MagLev) can be effectively utilized for various types of cells in cell culture and biofabrication applications. In line with this wide and effective use of magnetic levitation in biotechnology, this technique has been used to investigate various cell types for purposes such as detection and diagnosis (Goranov et al. 2020; Wychowaniec and Brougham 2022). Some examples of these are (Figure 4) weightlessness simulation studies with adipocytes (Sarigil et al., 2020), cancer (Durmus et al., 2015), blood (Deshmukh et al., 2021), bone cells (Sarigil et al., 2019).

Additionally, continuous flow has been applied to living cells, facilitating cell sorting based on single cell density (Kecili et al., 2023). The potential of the levitation system as a 3D biofabrication tool has been demonstrated through the 3D assembly of different cell types (Anil-Inevi et al., 2021). By altering the shape or configuration of the magnets, the applied magnetic field, system efficiency, and accuracy can be controlled, enabling precise manipulation of cells (Schuerle et al. 2013; Wang et al. 2020; Zhao et al. 2016). In this thesis, we applied magnetic levitation to keratinocytes for single cell density measurement and biofabrication, aiming to transfer magnetic levitation technology to the field of skin cell detection and skin tissue engineering.

Previous magnetic levitation studies have determined the density of various cell types such as cancer cells (1.044-1.084 g/ml) (Durmuş et al., 2015), bone marrow cells (1.07 g/ml) (Sarıgil et al., 2019), adipocytes (0.989 g/ml) (Sarıgil et al., 2020) and white blood cells (1.088 g/ml) and red blood cells (1.109 g/ml) (Durmuş et al., 2015). However, based on the literature, density determination by magnetic levitation has not been applied to keratinocytes before. This study aims to make this contribution to the literature by examining keratinocytes using magnetic levitation for the first time and to contribute to future skin cell studies. Understanding the biophysical properties of keratinocytes with this method may provide new insights and suggests that the label-free, scaffold-free magnetic levitation method may be a practical alternative for future research and applications in tissue engineering.
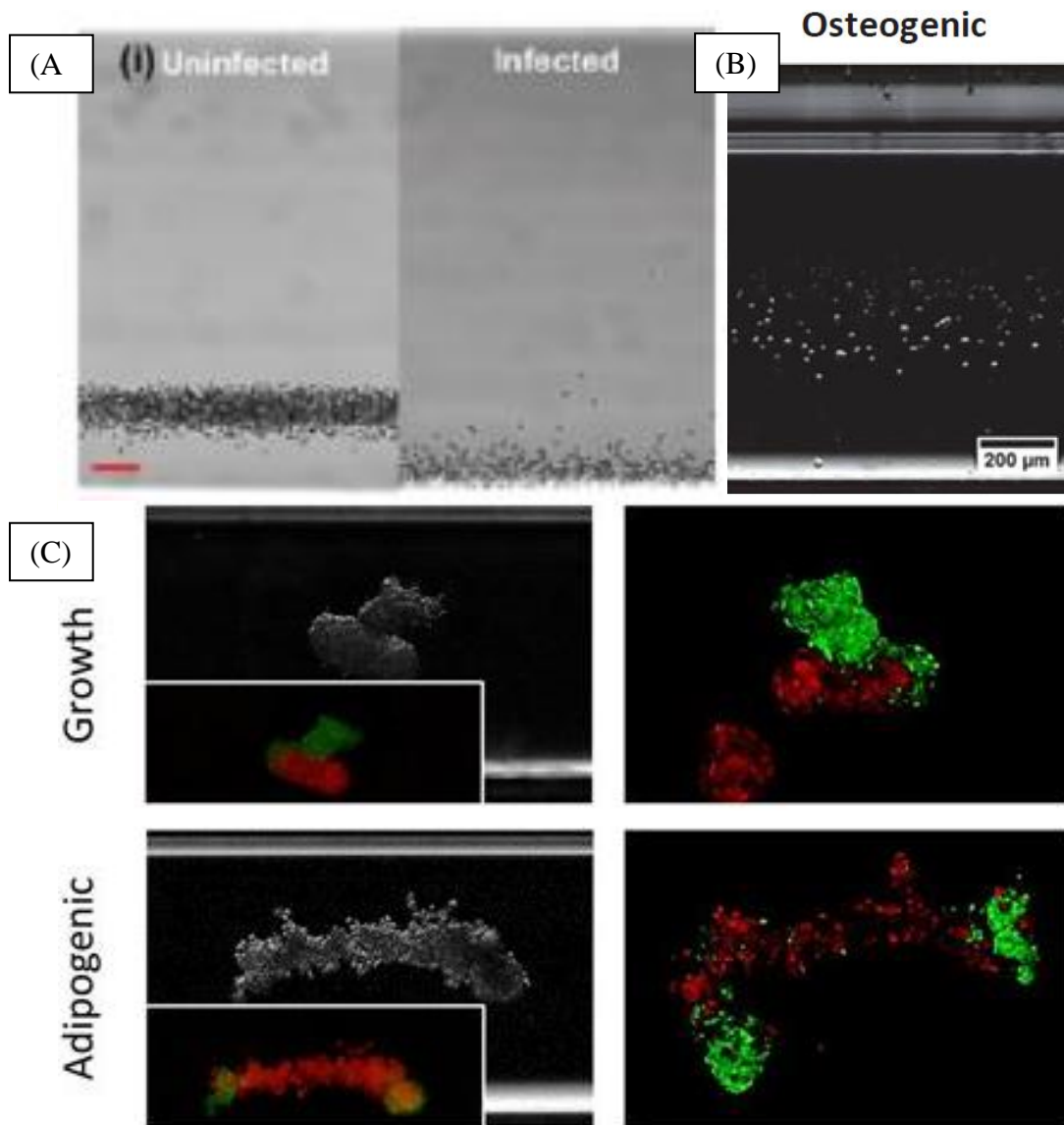
Figure 4. Various cell types have been subjected to magnetic levitation in previous studies in the literature. Examples include A) The application of magnetic levitation to blood cells (Source: Deshmukh et al., 2021) B) Levitation of bone cells from osteogenic differentiation of 7F2 cells (Source: Sarigil et al., 2019) C) Lipid cells from adipogenic differentiation, and the. This can thus serve various diagnostic purposes (Source: Sarigil et al., 2020).

1.2. Skin Tissue

The skin, the largest organ of the human body, plays multifaceted roles in protection, temperature regulation, sensation and even various physiological processes that are crucial for our general well-being (Yu et al. 2019) (Figure 5). In this context, beyond its visible functions in protecting against physical trauma, skin tissue plays a vital role in regulating body temperature through insulation and sweating mechanisms (Burns et al., 2010; Crucianelli & Ehrsson, 2022; Wysocki 1999). Furthermore, skin tissue serves as the primary interface for sensory perception, as it harbors receptors for touch, temperature, and pain (Baumbauer et al. 2015; Greenspan and Bolanowski 1996). In addition to these sensory functions, the skin is known to be an integral part of our immune defense system as it acts as a barrier against pathogens and harmful substances (Kolarsick et al., 201; Proksch, Brandner, and Jensen 2008). The skin also plays a very important role in synthesizing vitamin D, which is essential for general well-being and provides many protections such as bone health, the immune system and heart health (Lehmann, Querings, and Reichrath 2004; Piotrowska, Wierzbicka, and Żmijewski 2016). Its participation in transport processes is also vital, as it contributes to the overall metabolic balance by assisting in the excretion and absorption of essential substances (Jepps et al. 2013; Roberts, Pellett, and Cross 2002). Besides, as a protective barrier, the skin maintains internal homeostasis by protecting the body from external irritants, UV radiation and harmful chemicals. Complex network of nociceptors, thermoreceptors and mechanoreceptors in the skin forms an important component of our sensory system, enables us to perceive and respond to our environment (Green 2004; Kenton, Crue, and Carregal 1976; Lumpkin & Caterina, 2007). Understanding the complexity and importance of skin tissue lays the groundwork for exploring innovative approaches such as cell studies, cell culture methodologies and tissue engineering applications, and holds great promise for advancing healthcare and regenerative medicine. (Aleemardani et al. 2021; Eckert, Crish, and Robinson 1997; Hofmann et al. 2023; Rinn et al. 2008).
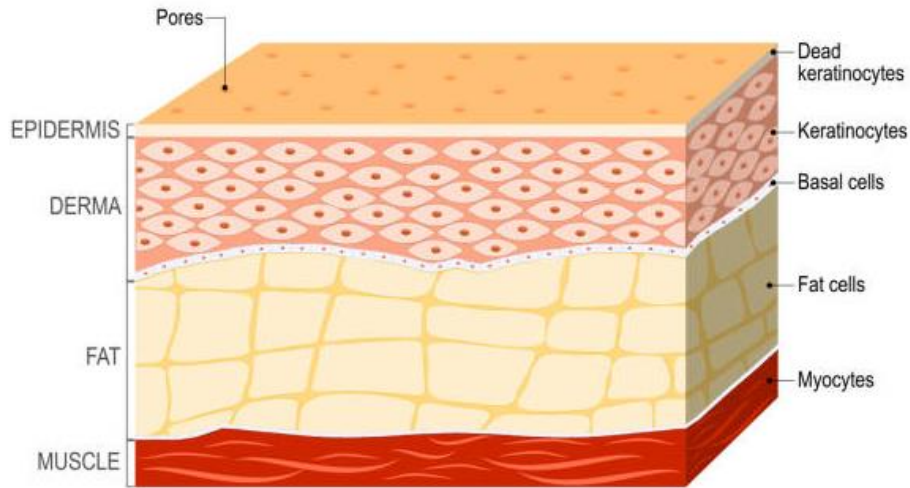
Figure 5. General representation of skin tissue layers, cell groups, and tissues present within them. (Source: Dermahelp™, 2022).

As mentioned earlier, magnetic levitation has been studied in various cell types, and as discussed above, skin has important characteristics for health. Therefore, we intend to use skin cells as models in our magnetic levitation studies. In particular, we plan to use utilize keratinocytes, which have not previously been studied in this context. Keratinocytes, as primary epidermal cells, will be central to the objectives of this project.

1.3. Keratinocytes

Keratinocytes serve as a fundamental model for studying skin biology due to their important role in maintaining skin integrity and function (Watt 2014). As the primary cells of the epidermis (Figure 6), keratinocytes contribute significantly to the structural framework of the skin by producing keratin proteins that provide strength and elasticity (C. Zhu et al. 2019; Elias et al. 2005 Quan et al. 2013). They play a crucial role in forming the previously mentioned skin barrier, which acts as a protective shield against environmental stressors and pathogens (Kirfel and Herzog 2004). Furthermore,

keratinocytes actively participate in dynamic processes such as wound healing and skin regeneration, where they regulate complex cellular interactions to promote tissue repair and restoration (Piipponen et al., 2020; Werner, Krieg, and Smola 2007). For example, during tissue repair, keratinocytes migrate to the site of injury, proliferate, and differentiate to facilitate wound closure and restoration of tissue integrity (Ramms et al. 2013; Vedula et al. 2013). In culture, keratinocytes exhibit the ability to express characteristic keratin proteins and organize them into stratified epithelial structures that closely resemble the architecture of the epidermis. Many studies have therefore exploited the unique properties of keratinocytes to gain valuable insights into skin physiology, pathology, and therapeutic interventions, making them indispensable tools for advancing our understanding of skin biology and disease mechanisms (Eckert, Crish, and Robinson 1997; Ratushny et al. 2012; Russo, Brembilla, and Chizzolini 2020; Yu et al. 2019)
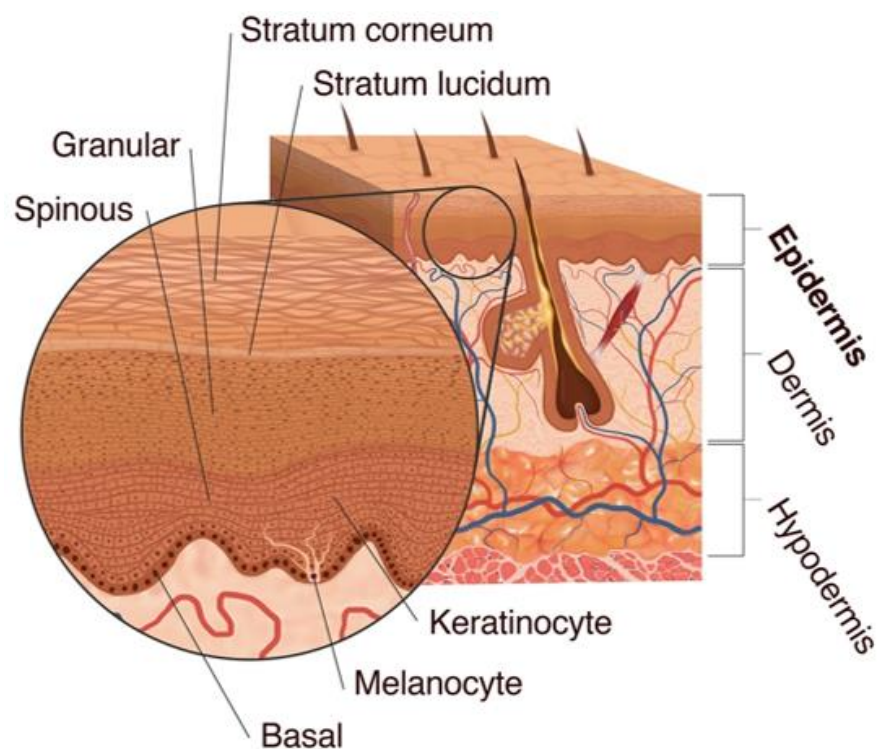
Figure 6. Layers of skin tissue are depicted. Essentially, from outermost to innermost: epidermis, dermis, and hypodermis layers. In a zoomed-in detail, examples such as keratinocytes and melanocytes are shown as cells located at the basal membrane of the outermost layer which called the epidermis (Source: Kern, 2022).

HaCaT cells, an immortalized human keratinocyte cell line, have emerged as a cornerstone in cell culture studies focused on understanding skin biology and related processes (Breitkreutz et al. 1993; Moran et al. 2021). Their widespread use in the scientific literature highlights their importance as a model system for investigating cellular behavior, particularly in contexts involving cell-cell communication. HaCaT cells provide a valuable platform for studying fundamental skin processes such as differentiation and wound healing that rely heavily on complex signaling pathways, including calcium signaling, as well as their intracellular interactions (Bakondi et al. 2003; Lee et al. 2005; Silva et al. 2017). Among these interactions, the interplay between calcium signaling and cell-cell communication is essential for regulating various keratinocyte functions, highlighting the interdependent nature of these pathways in modulating skin biology (Bikle et al., 2016). The use of HaCaT cells in research could elucidate the underlying mechanisms of these interactions, provide deeper insights into skin physiology and pathology, and pave the way for innovative approaches in therapeutic development and tissue engineering (Zheng et al. 2024).

A comprehensive understanding of these dynamic interactions leads to resolving the complexity of skin biology and has great potential to shed light on therapeutic interventions aimed at enhancing tissue regeneration and reducing cutaneous disorders (Gschwandtner et al. 2012; Mathes, Ruffner, and Graf-Hausner 2014; Niehues et al. 2018). Our study focuses on studying keratinocytes using four different HaCaT cell lines: MSCV, WT, D50Y and G45E. The D50Y and G45E groups represent different Connexin 26 mutations involved in rare genetic skin conditions, while MSCV contains an empty vector that acts as a control (Shuja et al., 2016). Each group represents specific genetic modifications or wild-type traits relevant to skin biology and disease. While the MSCV group acts as a control, the WT, D50Y and G45E variants allow us to explore how genetic alterations affect keratinocyte properties such as growth, differentiation and response to external stimuli. The culture of HaCaT cells serves as a valuable tool for studying various aspects of skin biology, including cell behavior, differentiation, and response to external stimuli, offering insights into physiological processes and disease mechanisms (Choi and Lee 2015; Pourzand, Albieri-Borges, and Raczek 2022).

1.4. Single Cell Density Determination

Single cell density, a critical cellular parameter, profoundly influences cellular behavior and physiological outcomes (Spetsieris and Zygourakis 2012; Spitzer and Nolan 2016). This metric encompasses fundamental aspects of cell morphology, size and spatial distribution within a defined area or volume (Grover et al. 2011). In studies, measuring single cell density can provide valuable insights into cell distribution patterns and population density, which are fundamental to understanding tissue organization and function (Da Silveira Dos Santos and Liberali 2018; Gomer, Jang, and Brazill 2011). Furthermore, cellular parameters, including single cell density, play a crucial role in improving our understanding of cell biology and disease progression (Chattopadhyay et al. 2014). In addition, changes in single cell density can influence processes such as differentiation, migration, and response to external stimuli, as they affect cell-cell interactions, signaling dynamics and overall tissue architecture. Incorporating single cell density analyses into experimental studies provides a quantitative framework to elucidate cellular behaviors and their impact on health and disease, thus contributing to the broader landscape of biomedical research and therapeutic development (Mathys et al. 2019; Trajkovic et al. 2019). This study is based on the magnetic levitation technique and equipment and system for measuring single cell density. As described in more detail in the materials and methods section, cells were cultured in a miniature magnetic levitation system in a paramagnetic environment. Real-time imaging is also possible in this system.

Cellular parameters encompass a range of properties such as cell morphology, size and other measurable attributes and provide valuable information about the structure, function, and behaviors of individual cells. Since one example of these parameters is single cell density, which is a very important metric that measures the number of cells in a defined volume or area. This measurement is important in elucidating cell distribution patterns in tissues or culture systems (de Vargas Roditi & Claassen, 2015). Furthermore, an accurate assessment of single cell density can provide a deeper understanding of cellular organization, proliferation dynamics and intercellular interactions that are fundamental to various physiological processes and disease states (Krishnaswamy et al. 2014; Longo et al. 2021). Moreover, these cellular parameters are indispensable tools to advance our understanding of cell biology and unravel the complex mechanisms

underlying disease progression (Jackson et al. 2020). Therefore, the study and characterization of cellular parameters, such as in the case of single cell density, plays a crucial role in fostering innovation and discoveries in various fields of biomedical research.

1.5. Tissue Engineering

Tissue engineering is a multidisciplinary field that focuses on developing biological substitutes with the aim of restoring, maintaining, or improving tissue function (Salgado et al. 2013). Tissue engineering combines the principles of biology, engineering and materials science and aims to create viable substitutes that can mimic the structure and function of natural tissues (Berthiaume, Maguire, and Yarmush 2011; Chandra et al., 2020). Tissue engineering applications cover a wide range of medical fields, including the regeneration of skin, bone, cartilage, and other tissues (Cancedda et al. 2003; Yu et al. 2019). This technology offers hope for the treatment of conditions such as burns, traumatic injuries and degenerative diseases (Lanza et al., 2020).

As components, advances in biomaterials, stem cell technology and bioprinting have further advanced the field by enabling the development of complex tissue structures and organoids (Chakraborty, Chawla, and Ghosh 2022). As a consequence, tissue engineering offers the potential for personalized medicine, providing tailored solutions that can significantly improve patient outcomes and quality of life (Neves et al. 2016).

1.6. Skin Tissue Engineering

Keratinocyte tissue engineering stands at the forefront of efforts to address the pressing need for effective skin tissue regeneration in a variety of clinical contexts (Bannasch et al. 2003; Vig et al. 2017; Zhong et al. 2022). The demand for skin replacement arises in scenarios such as severe burns, chronic wounds, traumatic injuries, surgical excisions, and various skin disorders where conventional treatments may fall

short (Dai, Shih, and Khachemoune 2020; Markiewicz-Gospodarek et al. 2022). In response to these challenges, skin implants have emerged as critical therapeutic interventions, encompassing autografts, allografts, xenografts, and synthetic skin substitutes (Vyas and Vasconez 2014) (Figure 7). However, limitations in donor availability, immune rejection, and long-term integration underscore the need for innovative tissue engineering approaches to overcome these hurdles (Chhabra, Sutherland, and Brayman 2014; Dixit et al. 2017; Kianian et al. 2023). By harnessing advances in biomaterials, scaffold design, and cellular therapies, tissue engineering endeavors aim to develop personalized and sustainable solutions for skin regeneration (Yu et al. 2019). These efforts hold the promise of revolutionizing clinical practice by enhancing the functionality, durability, and compatibility of skin substitutes (Figure 8), thereby improving outcomes for patients in need of skin repair and regeneration (Barros et al., 2021).
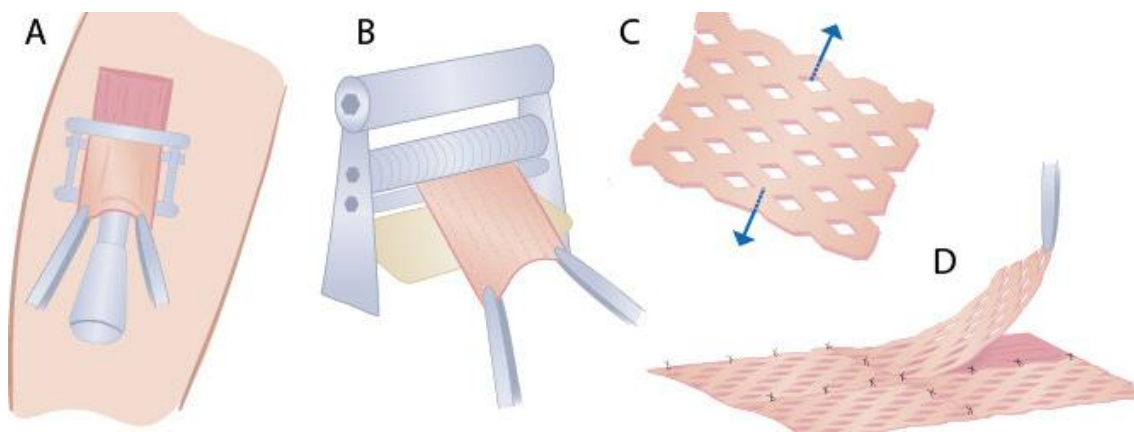
Figure 7. Step-by-step preparation of substitute tissues, using conventional methods, obtained from different donorship methods for replacing lost tissue in cases of skin tissue loss (Source: Khan et al., 2022).

Techniques in keratinocyte tissue engineering documented in the literature encompass a diverse array of methodologies aimed at mimicking the complex microenvironment of native skin tissue (Rijal and Li 2018; W. Wang et al. 2023). Cell culture conditions and co-culture systems are tailored to provide optimal growth and differentiation cues for keratinocytes, often in conjunction with other cell types, such as

fibroblasts or endothelial cells to emulate the physiological interactions observed in vivo (Jung et al. 2020; Pars et al. 2021). Bioreactors and mechanical stimulation platforms offer dynamic culture environments that simulate mechanical forces experienced by cells in vivo, promoting tissue maturation and functionality (Castro et al. 2020). Tissue printing and bioprinting techniques enable precise deposition of cells and biomaterials to create complex three-dimensional structures with spatial control, facilitating the fabrication of skin constructs with customized architectures (Augustine 2018). Decellularization and recellularization strategies involve the removal of cellular components from donor tissues followed by repopulation with keratinocytes and other relevant cell types, offering a natural extracellular matrix scaffold for tissue regeneration (Gilpin and Yang 2017; Mendibil et al. 2020). Biomaterial scaffolds, ranging from natural polymers to synthetic matrices, provide structural support and biochemical cues to guide cell behavior and tissue organization, serving as the foundation for engineered skin constructs (Guimarães, Marques, and Reis 2022; (Chaudhari et al. 2016; Shevchenko, James, and James 2009). Collectively, these advanced techniques represent innovative approaches to keratinocyte tissue engineering, offering unprecedented opportunities for the development of functional skin substitutes with enhanced biocompatibility, mechanical properties, and clinical efficacy (Figure 8).

As discussed, various skin tissue engineering techniques and studies offer promising solutions for tissue repair and replacement compared to conventional methods. These diverse techniques aim to address tissue loss and promote healing more effectively. However, as an alternative to these approaches, magnetic levitation provides a more economical, practical, and label-free method for tissue engineering and 3D biofabrication (Daquinag, Souza, and Kolonin 2013; Turker and Arslan-Yildiz 2018). This scaffold-free technique presents a novel and innovative approach to tissue engineering. In this study, we utilize magnetic levitation for tissue engineering applications. Therefore, the aims of our study are twofold. First, we aim to develop precise methods to measure keratinocyte density at the single cell level. This includes optimizing techniques to accurately measure cell density and assess variations between different HaCaT cell lines. Secondly, we aim to utilize MagLev technology for the biofabrication of 3D keratinocyte constructs. Using magnetic levitation, we aim to assemble these cells into structured, three-dimensional models that mimic their natural tissue. Our evaluation will focus on determining the structural integrity and functional capabilities of these constructs, aiming to advance tailored tissue engineering applications for dermatological and biomedical purposes.
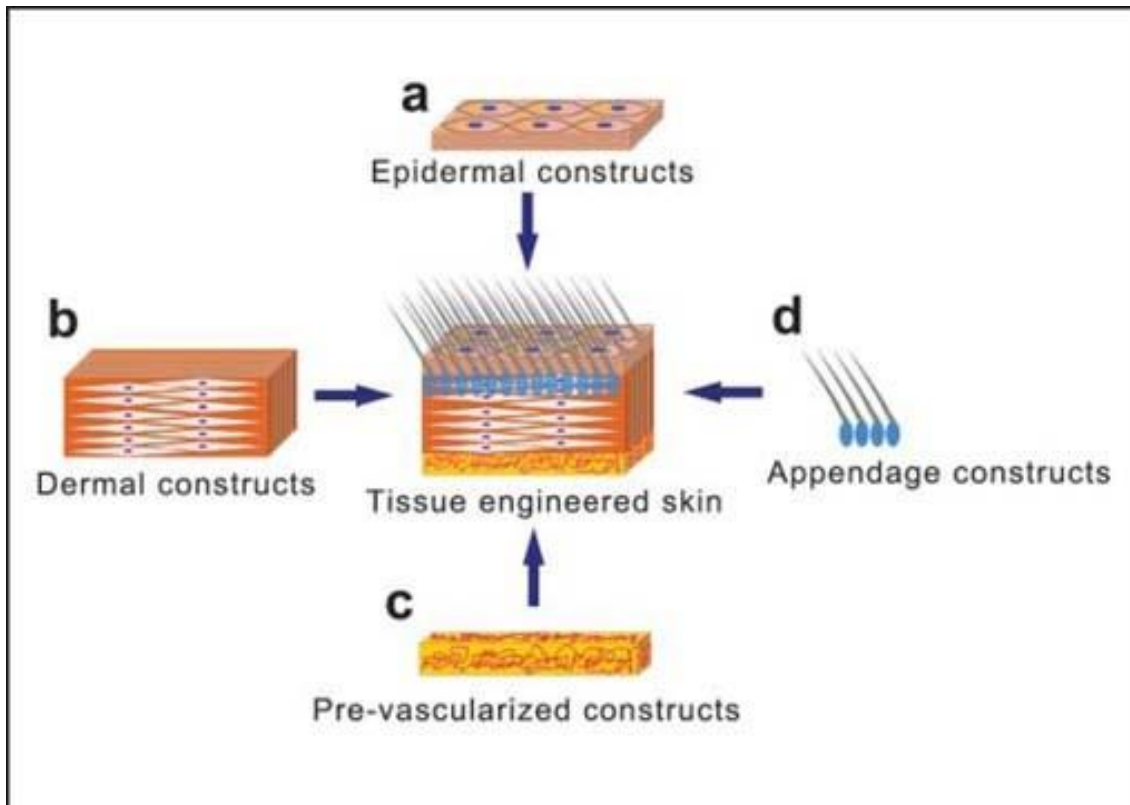
Figure 8.   Separate components that can be individually designed in the construction of
skin tissue through tissue engineering (Source: Jin & Bi, 2013).

CHAPTER 2

MATERIALS AND METHODS

2.1. Magnetic Levitation Platform and Experimental Setup

In the magnetic levitation system, magnetic fields counteract the gravitational forces and thus allow cells to levitate inside the paramagnetic medium without any physical contact. In this environment, the movement of the cells is towards the lower magnetic field. The basic concept involves balancing two main forces: magnetic force (Fmag) and corrected gravitational force (Fg), which is a combination of gravitational and buoyancy forces (Figure 9). Hence, these forces to provide magnetic levitation are expressed by the following equations (Eq 1 and Eq 2), respectively. For the magnetic force, which is the dominant force, V is the cell volume, delta χ is the magnetic susceptibility difference between the paramagnetic medium and the cell, $\mu 0$ is the permeability of free space and B is the magnetic induction. For the corrected gravitational force, where delta ρ is the density difference between the paramagnetic medium and the cell and g is the gravitational acceleration (Sarigil et al., 2019).

$$F_{mag=\frac{V\Delta_X}{\mu_0}(B.\nabla)B} \quad (Eq\ 1)$$

$$F_g = V.\Delta\rho.g \quad (Eq\ 2)$$
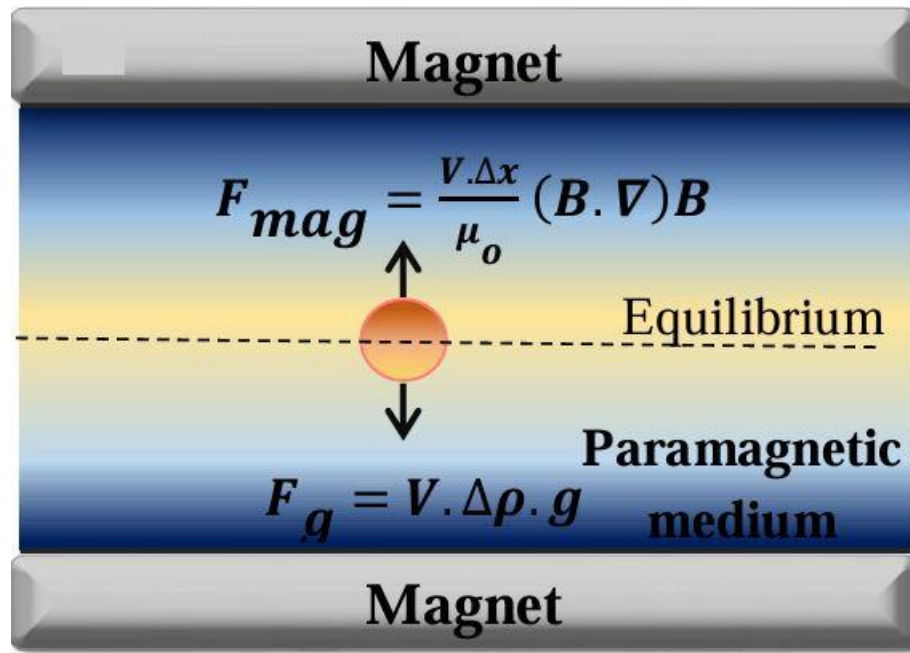
Figure 9. Representation of forces present and in equilibrium within the magnetic levitation system. (Source: Sarigil et al., 2019).
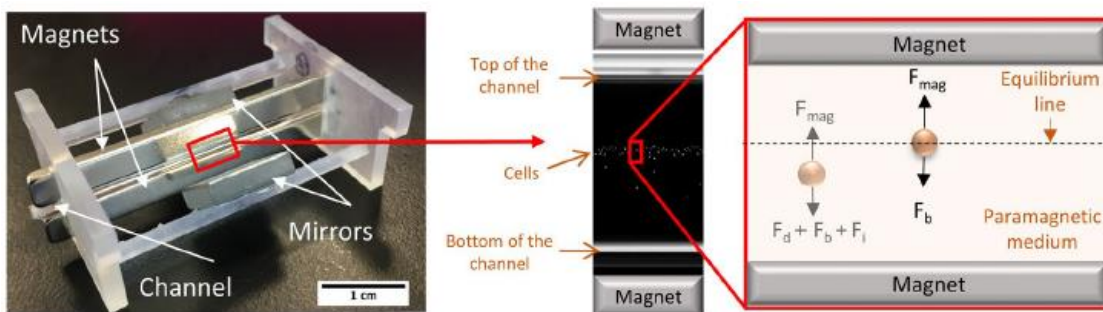
Figure 10. Magnetic levitation setup and the fundamental principles involving the forces at play. Fluidic drag force (Fd), inertial force (Fi), buoyancy force (Fb) and magnetic force (Fmag) (Source: Anil-Inevi et al., 2018).

In accordance with these principles, design of the magnetic levitation platform is achieved for levitation of cells based on density (Figure 10). The platform consists of two N52-grade neodymium magnets (NdFeB, Supermagnete) arranged with like poles

opposing each other, a microcapillary channel (Vitrocom), and two mirrors set at a 45˚ angle for real-time cell imaging. The loaded in microcapillary channels are levitated in a paramagnetic medium (Gadavist®, Bayer, Gd^{3+}). The components of the magnetic levitation platform are assembled using handles produced through a 3D printer.

2.2. Cell Culture

Culturing HaCaT cells, an immortalized human keratinocyte cell line, involves techniques to ensure their robust growth and maintenance in vitro. HaCaT cells are cultured in a growth medium, such as Dulbecco's Modified Eagle Medium (DMEM) supplemented with 10% fetal bovine serum (FBS, Biological Industries) and antibiotics; 1% penicillin/streptomycin (Invitrogen) which provide essential nutrients and support cell proliferation. Additionally, the culture environment is maintained at optimal conditions, including a humidified atmosphere with 5% CO2 at 37°C, to support cell viability and functionality HaCaT cells are routinely passaged upon reaching confluence to prevent overcrowding and maintain their proliferative capacity. Passaging involves detachment of cells from the culture vessel using 0.25% trypsin/EDTA solution (Biological Industries) for 5 minutes when they reach approximately 80-90% confluence (every 4-6 days), followed by reseeding at a lower density to facilitate continued growth. Medium was refreshed every 2-3 days and the cell morphology and viability were regularly monitored to ensure the integrity of the cell culture. HaCaT cells were infected with an MSCV retroviral vector containing the cDNAs for Cx26-WT, Cx26-G45E, and Cx26-D50Y. The groups of cells infected with these vectors were designated as WT for MSCV-Cx26-WT, G45E for MSCV-Cx26-G45E, and D50Y for MSCV-Cx26-D50Y throughout the thesis. The empty MSCV vector was used as a control and referred to as MSCV. To ensure hemichannels remained closed and to support cell growth, 3.2 mM $CaCl_2$ was added to the medium of the infected HaCaT cells.

2.3. Magnetic Levitation of the HaCaT Cells

4 groups of HaCaT cells maintained in cell culture followed by magnetic levitation is the basis of the planned methodology.

Calcium, which is normally added for cells to attach to the plate bottom, was not added to the medium prepared for levitation. 4 different groups were used. These were: MSCV, Wild Type, D50Y and G45E groups. cells cultured in growth and adipogenic induction medium were trypsinized with 0.25% trypsin/EDTA solution and the cell suspension was centrifuged (Eppendorf) at 1.1 rcf for 5 min. The pellet was resuspended to 10^5 cells/mL in the culture medium and each sample with 50 μl per capillary (5000 cells/capillary) were loaded into the microcapillary after adding Gd^{3+} paramagnetic agent with concentrations of 15 mM, 30 mM, 50 mM, 100 mM and 200 mM. When the cells reached the equilibrium position within 8 min, the levitated cells were imaged under an inverted microscope. Cells that are cultured by magnetic levitation in a miniaturized system that provides levitation between two magnets. Levitated cell culture, cellular pattern under simulated weightlessness, gives opportunity for real-time imaging at this point. Imaging of the cells was conducted at 10× magnification under an inverted microscope.

2.4. Magnetic Levitation of Polymeric Beads

Polymer beads with different densities, 1 g mL^{-1}(with size of 10–20 μm), 1.035 g mL^{-1}(with size of 38–45 μm), 1.07 g mL^{-1}(with size of 10–20 μm) and 1.09 g mL^{-1}(with size of 20–27 μm) (Cospheric LLC., ABD), were levitated in the culture medium containing 15 mM gadolinium (Gd^{3+}) (Gadavist®, Bayer) to calibrate the density gradient of the magnetic levitation device. Levitated beads were visualized at 4× under an inverted microscope (Olympus IX-83) after beads reached the equilibrium position (within ~10 min) in the magnetic levitation platform. The levitation heights of the beads (distance from the upper limit of the bottom magnet) were determined using the ImageJ Fiji software.

2.5. Biofabrication of the 3D Structures

2.5.1. Cell Culture in Magnetic Levitation for 3D Structures

In this part of the study, HaCaT cells from four different groups (MSCV, WT, D50Y, G45E) were subjected to magnetic levitation using the same magnetic levitation device system and technique in previous single cell density measurement experiments. Unlike previous experiments focusing on single cell density determination, the cells were allowed to levitate for varying durations of 24 hours and 48 hours and 72 hours to observe the formation of three-dimensional (3D) structures. Also; 200 000 cells/capillary was used in this section. Additionally, different concentrations of gadolinium (Gd^{3+}) were utilized to optimize the levitation process. Specifically, a concentration of 50 mM Gd^{3+} was found to yield superior results, with the observed 3D structures positioned more centrally within the capillary. In contrast, when using a lower concentration of 30 mM Gd^{3+}, the structures tended to adhere and accumulate along the sides of the capillary. These experimental parameters were systematically adjusted to evaluate the influence of magnetic levitation duration and Gd^{3+} concentration on the spatial organization and morphology of HaCaT cell aggregates within the levitated environment.

2.5.2. Cell Culture on Agarose Gel for 3D Structures

At this point of the study, HaCaT cells were cultured in a 96-well plate pre-filled with agarose gel to facilitate the formation of three-dimensional (3D) structures. The agarose gel was prepared by mixing 26 mg of agarose powder with 13 mL of DMEM (Dulbecco's Modified Eagle Medium), followed by autoclaving to ensure sterility. After the gel was allowed to cool slightly but remained in a liquid state, 500 µL of the gel was combined with 500 µL of serum-free DMEM in Eppendorf tubes. This mixture was swiftly transferred to each well of the 96-well plate, with 30 µL dispensed into each well to form a solidified gel layer. It was crucial to speed up this process to prevent the agarose

gel from solidifying prematurely. The reason for choosing serum free medium is that the cells form 3D structures within themselves without sticking to agarose (as they stick to the plate).
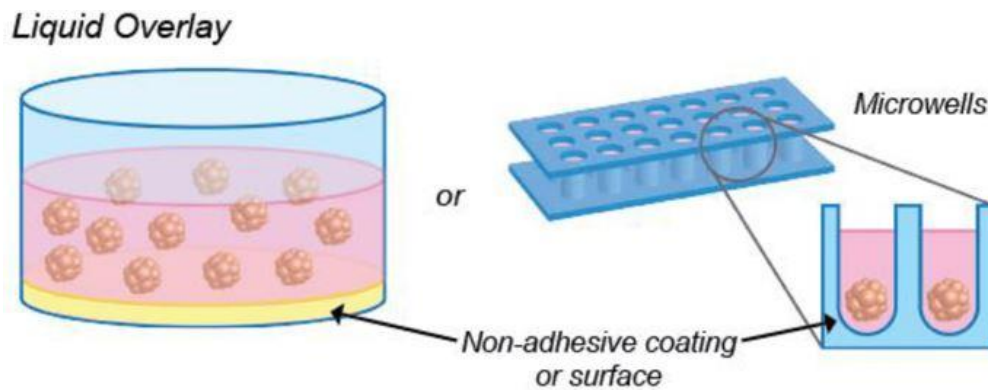
Figure 11. Cell seeding onto agarose gel using the liquid overlay method. The conventional method (Source: Van Zundert et al., 2020).

Once the agarose gel-containing 96-well plate was ready and cooled, three-dimensional structures (previously incubated in a magnetic levitation system for 24 hours) were transferred from capillaries into the wells. The structures were then allowed to further develop and interact within the 3D environment provided by the agarose gel. After 24 hours, the 3D structures within the agarose gel wells were observed and analyzed.

As control experiments, HaCaT cells were directly transferred into agarose gel without prior magnetic levitation. Comparatively, the results demonstrated that magnetic levitation significantly facilitated the formation of spherical 3D structures within the agarose gel wells, indicative of enhanced cellular organization and interactions. These findings highlight the potential of magnetic levitation as an alternative approach for promoting cellular aggregation and structuring in tissue engineering applications.

2.6. Statistical Analysis

Statistical analysis of data obtained from images of HaCaT cells undergoing magnetic levitation experiments involves processing using image analysis software such as ImageJ. Initially, images captured with a light microscope are imported into the software for analysis. Then, the analysis of levitation images of the cells was done via Image J Fiji software to determine levitation heights, density and cell size. In the results of the bead calibration experiments, graphs showing the levitation height versus bead density at different Gd^{3+} concentrations were plotted. and linear regression was performed on the data to obtain equations that provide the particle/cell density levitated in the magnetic sensing system. Also, for biofabrication part, various parameters such as cell area, perimeter, density, and morphology were quantified using ImageJ's toolset. Through segmentation techniques, individual cells can be separated from the background, enabling precise measurements of cellular features. Statistical analyses, including mean values, standard deviations, and histograms, provided insights into the distribution and variability of cell properties within the sample population. Additionally, comparative analyses between control and experimental groups were performed to assess the effects of magnetic levitation on HaCaT cell behavior and morphology. One-way ANOVA with Tukey's multiple comparisons test was used and $p < 0.05$ was considered as statistically significant.

CHAPTER 3

RESULTS AND DISCUSSION

3.1. Cell Culture

Initially, four different HaCaT groups were cultured in a medium containing Ca^{2+}. Calcium (Ca^{2+}) was added to the medium because it is known that groups with connexin26 (Cx26) mutations form hyperactive hemichannels that disrupt calcium (Ca^{2+}) transfer (Gerido et al. 2007; Yasarbas et al. 2024). Ca^{2+} is critical for normal epidermal cell function, and without it, proper culture and passage are not possible. To ensure cell adhesion to the petri dish surface and to maintain ongoing culture work, Ca^{2+} was included in the medium.
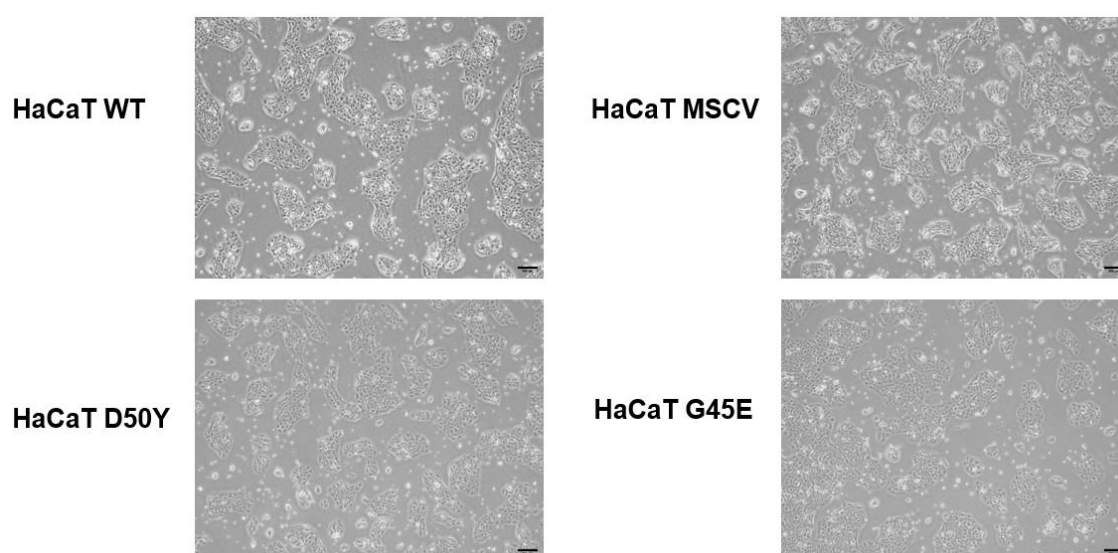
Figure 12. 2D Cell Culture images of 4 different HaCaT groups: Wild Type, MSCV, D50Y, G45E medium for 5 days. Scale bar: 200 μm.

When all cells were cultured in a medium containing Ca^{2+}, similarities in morphology were observed between control groups Wild Type (WT) and MSCV, G45E and D50Y cells (Figure 12). However, cultures of G45E and D50Y mutants exhibited greater difficulty in detachment after trypsinization when passaging to new plates.

3.2. Gadavist Concentration Optimization

Gadavist concentration optimization was performed using MSCV HaCaT cells. After cell culture in medium containing Ca^{2+}, the cells were levitated using a magnetic levitation device with Gadavist concentrations of 15 mM, 30 mM, 50 mM, 100 mM, and 200 mM. The choice of this concentration range and paramagnetic agent was for avoiding from the cytotoxic effects of Gd^{3+}, a lanthanide metal (Rogosnitzky and Branch 2016). The prevention from the cytotoxicity of Gd^{3+} can be done by using its chelated forms. Based on previous studies that examined the impact of different chelating forms on cell proliferation and the toxic thresholds of Gd^{3+}, this study employed a nontoxic concentration range (≤ 200 mM) and a nonionic, macrocyclic chelate form (Gadobutrol, Gadavist®) of Gd^{3+} (Anil-Inevi et al. 2018; Guo, Yang, and Zhang 2018).

As the Gd^{3+} concentration increased, the paramagnetic properties of the medium also increased, correlating with an observed increase in levitation height of the cells (Figure 13 a)., as depicted in the graph (Figure 13 b). Based on these results, concentrations of 15 and 30 mM were deemed suitable for single cell density measurements, and further experiments were conducted with other HaCaT cell groups. The levitation height values of MSCV were examined at different Gd^{3+} concentrations, resulting in the following measurements: 664.5 μm at 15 mM, 777.6 μm at 30 mM, 920.8 μm at 50 mM, 1034 μm at 100 mM, and 1157 μm at 200 mM. When comparing the increase in levitation heights, the results showed a respective rise of 17% at 30 mM compared to 15 mM, 39% at 50 mM compared to 15 mM, 56% at 100 mM compared to 15 mM, and 74% at 200 mM compared to 15 mM. Additionally, there was an 18% increase at 50 mM compared to 30 mM, a 33% increase at 100 mM compared to 30 mM, and a 49% increase at 200 mM compared to 30 mM. Further comparisons revealed a 12% increase at 100 mM compared to 50 mM and a 26% increase at 200 mM compared to 50

mM. Comparing 200 mM and 100 mM showed a 12% increase at 200 mM. As a result, 15 mM and 30 mM were selected as the optimal concentrations. This decision was based on both numerical data (Figure 13 b) and the analysis of levitation images (Figure 13 a), ensuring cell viability, accurate measurements, and ease of observation. These concentrations provided the best balance for maintaining healthy cells, obtaining precise measurements, and facilitating clear visual monitoring during the experiments.

Comparative analysis of four HaCaT cell lines (MSCV, WT, D50Y, G45E) revealed significant differences (Figure 14). The Tukey test detected significant differences, especially in the G45E group at 15 mM Gd^{3+} concentration, emphasizing its differential response under these conditions. In contrast, comparisons between MSCV and G45E at 30 mM Gd^{3+} concentration yielded non-significant results. In levitation height measurements, multiple comparisons revealed that statistical significance was defined as $p < 0.0001$ across all groups at a concentration of 15 mM. However, at the concentration of 30 mM, statistical significance was also defined as $p < 0.0001$ for all groups except for the MSCV and G45E groups ($p = 0.97$, depicted as b) (Figure 14). These findings indicate that further investigations using the 15 mM concentration are required to further elucidate the specific properties and behavior of different HaCaT cell lines. This study highlights the importance of standardization and reproducibility in experimental protocols to ensure robust and reliable results in magnetic levitation studies of HaCaT cells.

When the HaCaT cells were levitated in medium containing 15 mM Gd^{3+}, the average levitation height of the MSCV WT group was 7.048 μm lower compared to the control, representing a 1% decrease. In contrast, the D50Y group exhibited a decrease of 38.04 μm in levitation height compared to MSCV, corresponding to a 6% reduction. However, the G45E group showed a significant increase in levitation height by 188.8 μm compared to MSCV, marking a 29% increase. Since the results obtained with 15 mM Gd^{3+} were more reliable, we decided to conduct further experiments and evaluations using this concentration.
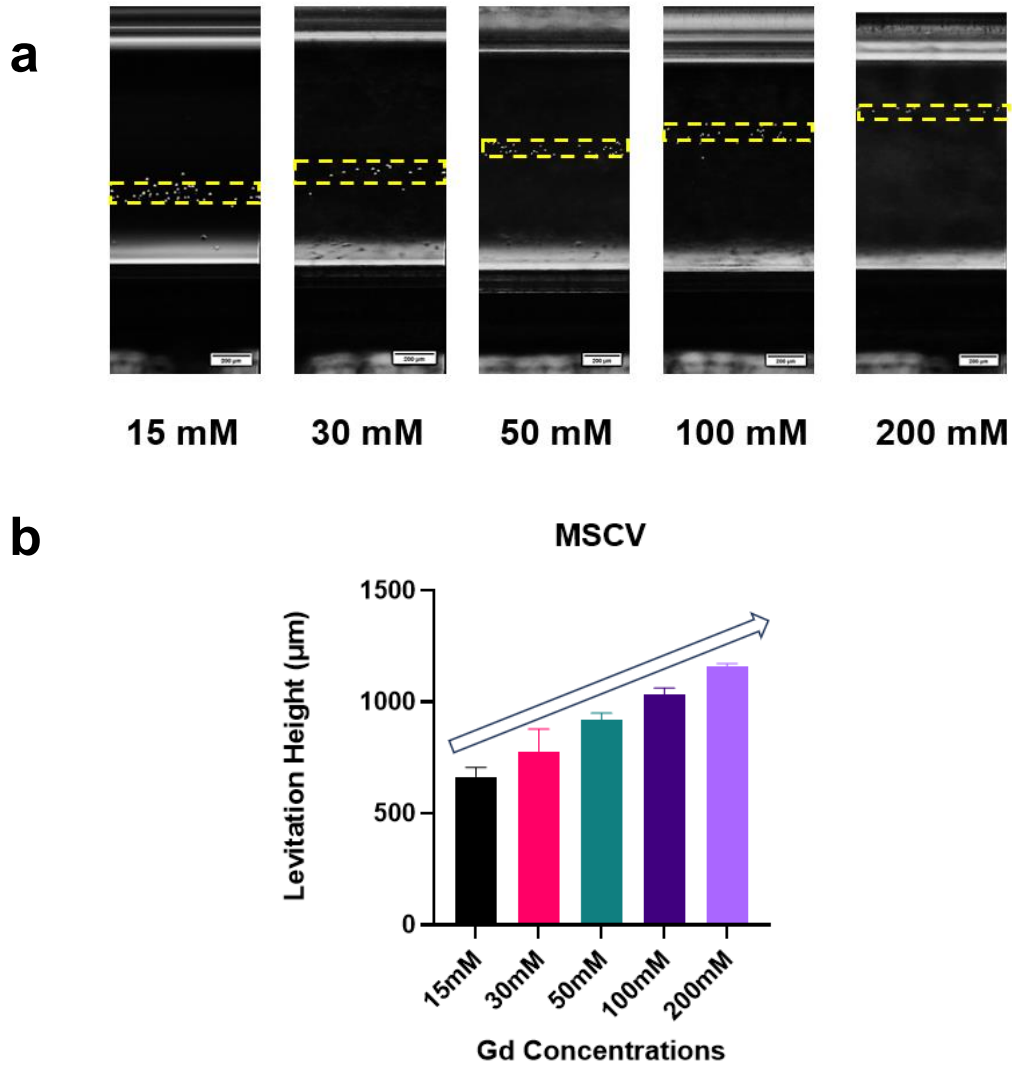
Figure 13. Levitation Height Measurements of Different Groups a) Levitation heights of HaCaT MSCV group at varying Gd^{3+} concentrations. Optimization of Gd^{3+} concentration was performed with 15, 30, 50, 100, and 200 mM. Yellow dashed lines indicate the positions of the Scale bar: 200 μm b) Graph of the relationship between levitation height and Gd^{3+} concentration. As Gd^{3+} concentration increases, levitation height also increases. Statistical significance was defined as: $p < 0.0001$ in all groups.
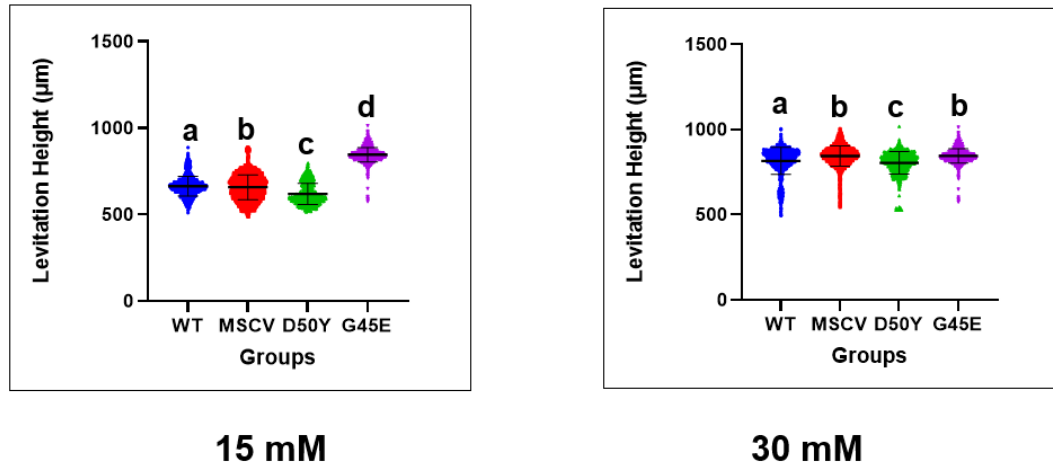
Figure 14. Comparison of levitation heights at 15 mM and 30 mM Gd^{3+} concentrations for four different HaCaT groups, shown on the graphs. Statistical significance was defined as: $p<0.0001$ in all groups in 15 mM. but 0.97 b groups (MSCV and G45E) in 30 mM.

3.3. Calibration of the Setup with Polymeric Beads

In our study, the magnetic levitation setup was calibrated using polymeric beads of known densities: 1.090 g/ml, 1.07 g/ml, 1.035 g/ml, and 1 g/ml. The beads were levitated in a 15 mM Gd^{3+} concentration to establish a reliable calibration curve. As expected, the beads' levitation heights were inversely proportional to their densities. When the density of the beads decreased, their levitation heights, defined as the distance from the upper surface of the bottom magnet, increased at a concentration of 15 mM Gd^{3+}. This calibration allowed us to translate levitation heights into accurate density measurements for the keratinocyte cells. The yellow dashed lines in the figure indicate the precise positions of the beads within the magnetic field, serving as reference points for the calibration process (Figure 15). Data are presented as mean ±SD (Figure 16). This calibration was crucial for the accurate assessment of single cell densities in our subsequent experiments.

Bead calibration values demonstrated the following average levitation heights for beads at different concentrations: 1154.71674 μm for 1 g/ml, 1045.758597 μm for 1.035

g/ml, 790.8774138 μm for 1.07 g/ml, and 649.855908 μm for 1.09 g/ml (Figure 16).

Based on the average density and levitation height values, an inverse relationship between density and levitation height was demonstrated, with linear equations obtained for the 15 mM Gd³⁺ concentration (Figure 16). The linear equation, which allows calculation of density using the levitation heights of single cells, showed a strong correlation with $\rho = -0.0001689 \times h + 1.203$ ($R^2 = 0.9687$); where ρ represents the density (g/mL) and h represents the levitation height (μm) for 15 mM Gd³⁺.
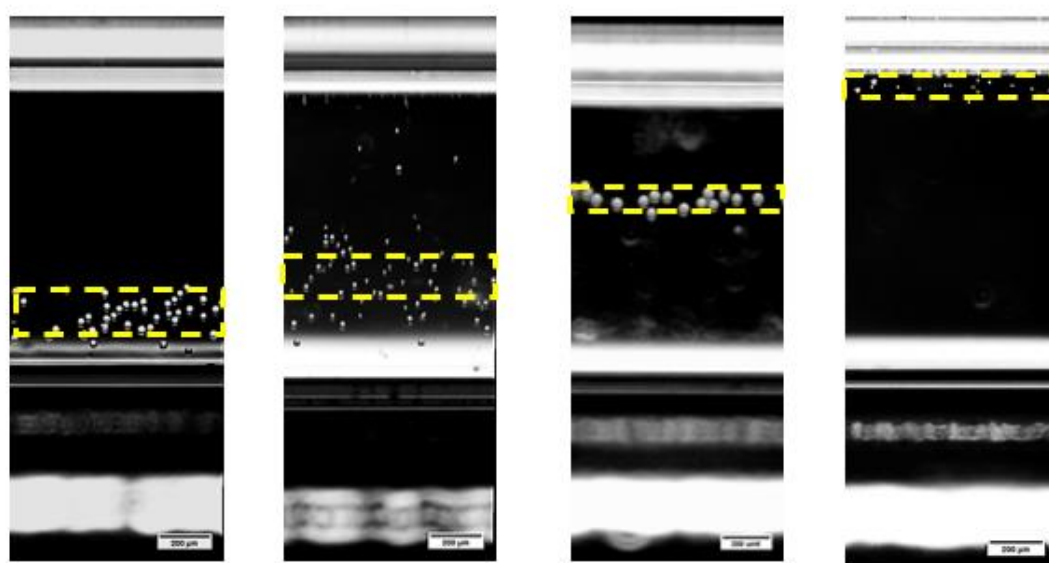
Figure 15. Calibration of the levitation system using beads with known densities. Magnetic levitation performed at 15 mM Gd³⁺ concentration. Beads with densities of 1.090 g/ml, 1.07 g/ml, 1.035 g/ml, and 1 g/ml levitate inversely proportional to their densities in the magnetic field. Yellow dashed lines indicate the positions of the beads. Scale bar: 200 μm.
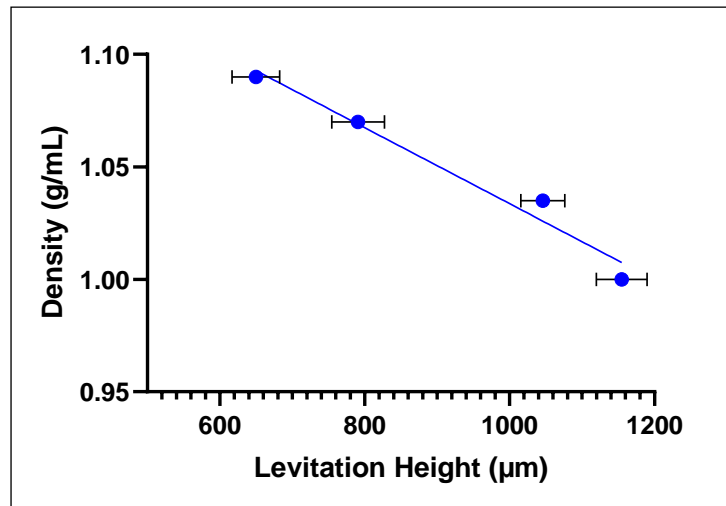
Figure 16. Levitation heights of polymeric beads with known densities. Data are presented as the mean of replicates with error bars (±SD). One way ANOVA with Tukey's multiple comparisons test was performed for statistical analysis of density- levitation height data.
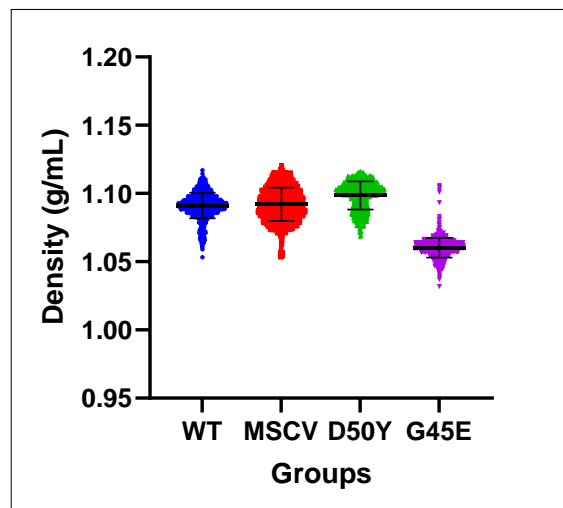
Figure 17. Density value transformation from the levitation height values of the four HaCaT groups: WT, MSCV, D50Y, G45E in 15 mM Gd^{+3} concentration. Significantly low density value of G45E group is shown. Data are presented as the mean of replicates with error bars (±SD). One way ANOVA with Tukey's multiple comparisons test was performed for statistical analysis. Statistical significance was defined as: $p < 0.0001$ in all groups.

The results of bead calibration enabled us to convert the levitation values of the four HaCaT groups into density values. This provided the distribution of density values, measured in g/ml, for each of the four groups (Figure 17).

The average density values for HaCaT groups were determined as follows: WT: 1.091 g/ml, MSCV: 1.092 g/ml, D50Y: 1.099 g/ml and G45E: 1.06 g/ml. The marked difference observed in the levitation heights of the G45E group was also evident in the density values, which were significantly lower compared to the other groups. This significant deviation in the G45E group not only highlights a potential anomaly but also points to an important diagnostic indicator. This finding may provide valuable information for further diagnostic developments.

3.4. Agarose Experiments

When HaCaT cells were added to 96-well plates prepared by pouring agarose gel, the formation of 3D structures by the gold standard method, as expected, did not observe spherical shapes in a very compact and uniform structure. The clustering behavior of HaCaT cells was observed by seeding them into a 96-well plate filled with agarose gel. In wells containing both medium and agarose gel, cells positioned on the surface of the agarose did not form significant aggregated structures from the first day. There was no tendency to form a single spherical shape. By the end of the fifth day, small, scattered clusters were still present. Increasing the cell concentration per well resulted in dispersed formations across all four groups. When seeded alone in agarose gel, the cells failed to form uniform, three-dimensional structures. In fact, dispersed settlements of cell clusters were observed. Initially, when working with 10 000 cells per well, the structures shown in (Figure 18) were obtained. Then, when the cell concentration was increased and 200 000 cells were used for each well, the shapes in (Figure 19) were formed, although they were in different order and pattern each time, a single spherical shape and bulk structure could not be achieved. As a result, the idea of transferring the cultures to agarose after cell culture by magnetic levitation was further supported. Because methods such as liquid overlay, which is the gold standard alone, were not sufficient to form the expected structure.
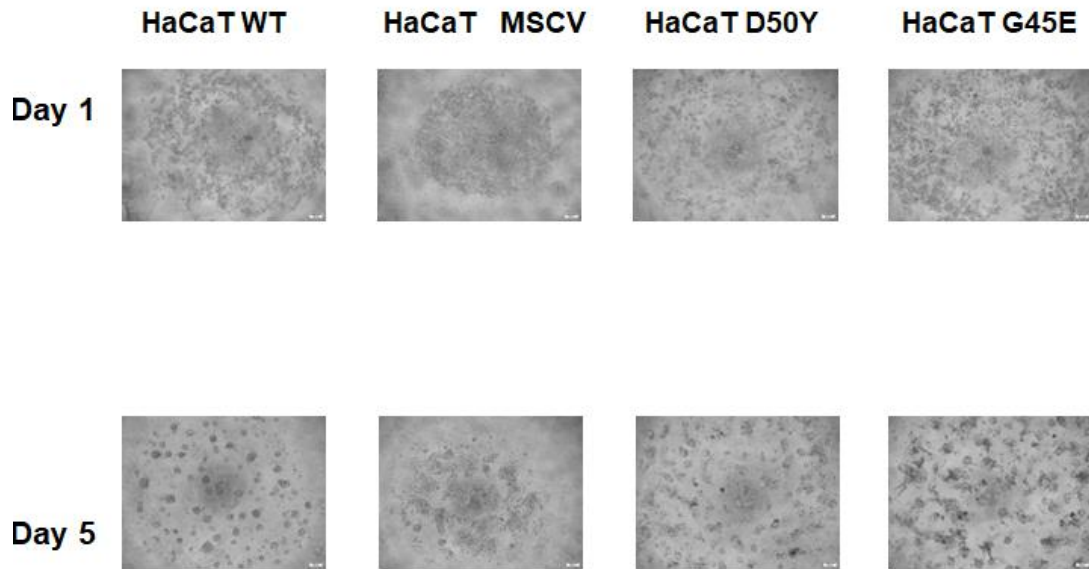
Figure 18. Agarose experiments with 10 000 cells in each well. Each group displayed a dispersed structure. Scale bar: 200 μm.
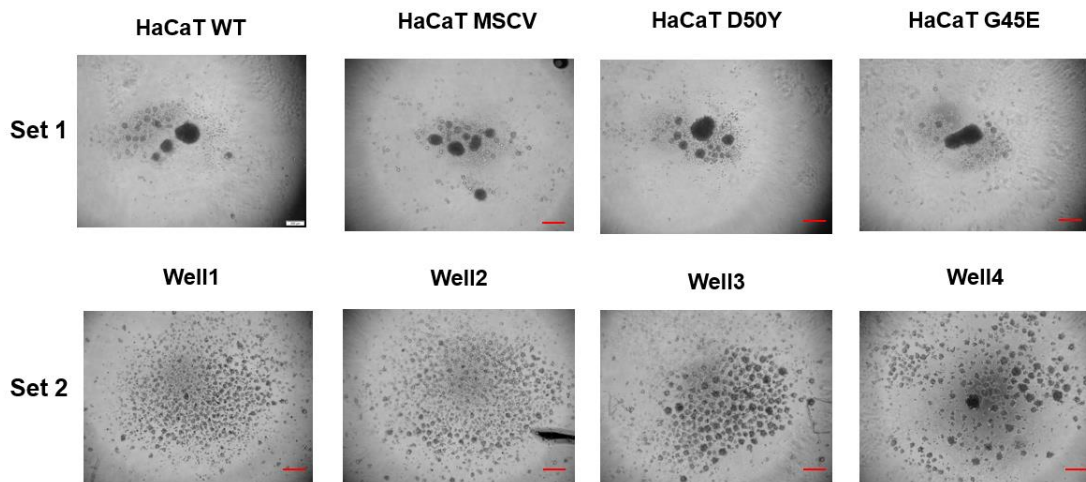
Figure 19. Agarose experiments with 200 000 cells in each well. Each group displayed a dispersed structure even at higher cell concentrations.

3.5. Culture in Magnetic Levitation

For magnetic levitation culturing experiments, Gd^{3+} concentrations of 30 mM and 50 mM were considered appropriate. This is both suitable for preventing the cells from sticking to the capillary glass in culture and is considered optimum for cell viability and health. However, cell structures adhering to the capillary glass at 30 mM Gd^{3+} concentration in both MSCV and G45E groups showed that this concentration was not suitable (Figure 20). Therefore, the experiment was continued with 50 mM Gd^{3+} concentration in the other groups. These results were obtained by keeping the culture in the magnetic levitation system for 1 day.
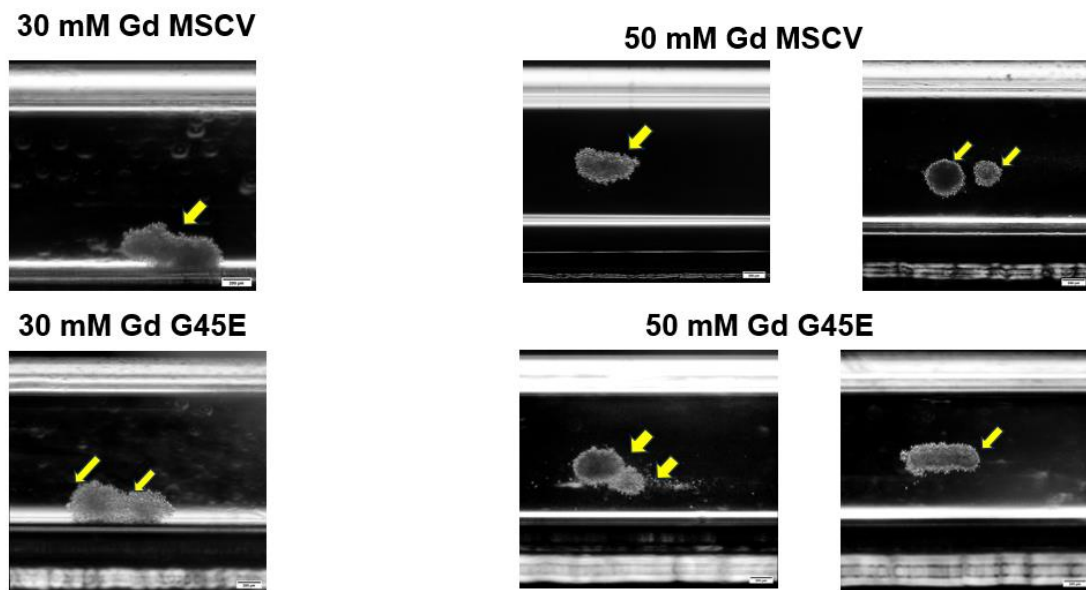
Figure 20. Cultures in device with 200 000 cells in each capillary. At 30 mM Gd^{3+} concentration, both MSCV and G45E groups showed structures adhered to the capillary, while at 50 mM, the structures were levitated.

After that, cell images were taken with fluorescence microscopy for 5 days in order to show that they lived in the magnetic levitation culture for more than 1 day, and at the end of the 5th day, it was observed that the cells maintained their form. The cells

also continued to live and did not form any flow in the capillary at the end of the 5th day (Figure 21).
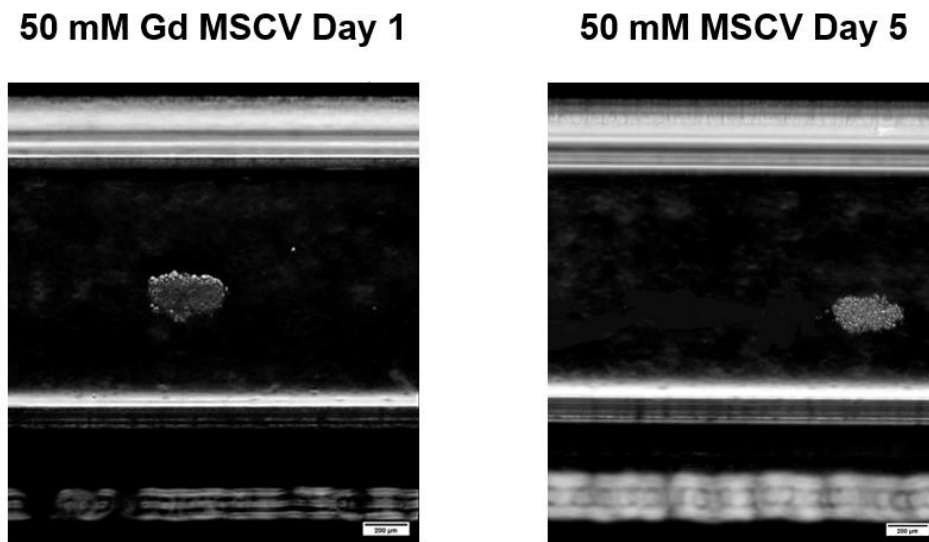
Figure 21. Images of MSCV cells in the capillary at 50 mM Gd^{3+} concentration on days 1 and 5. MSCV cell group cultured under magnetic levitation survived until day 5 without observable flow.
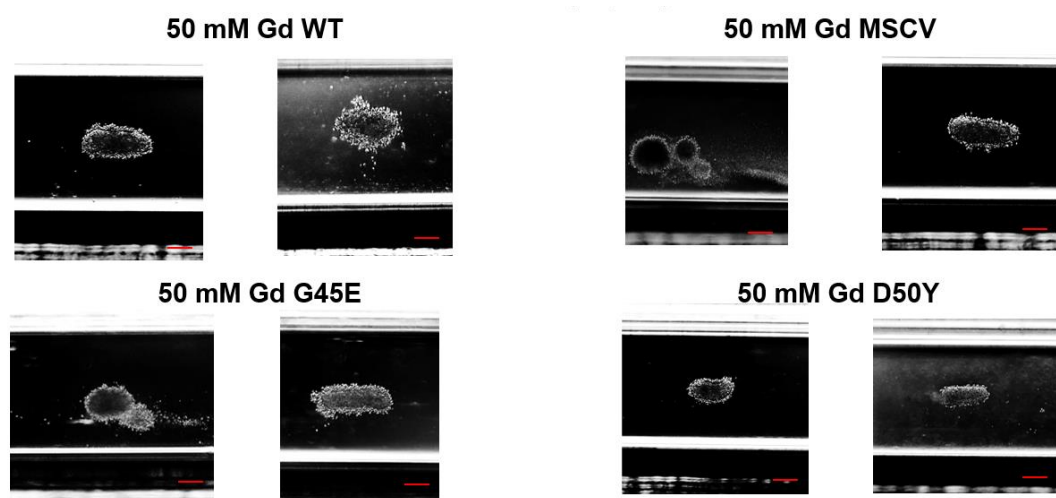
Figure 22. Culturing of the four different groups using magnetic levitation and imaging after 24 hours. Compact structures are observed.

32
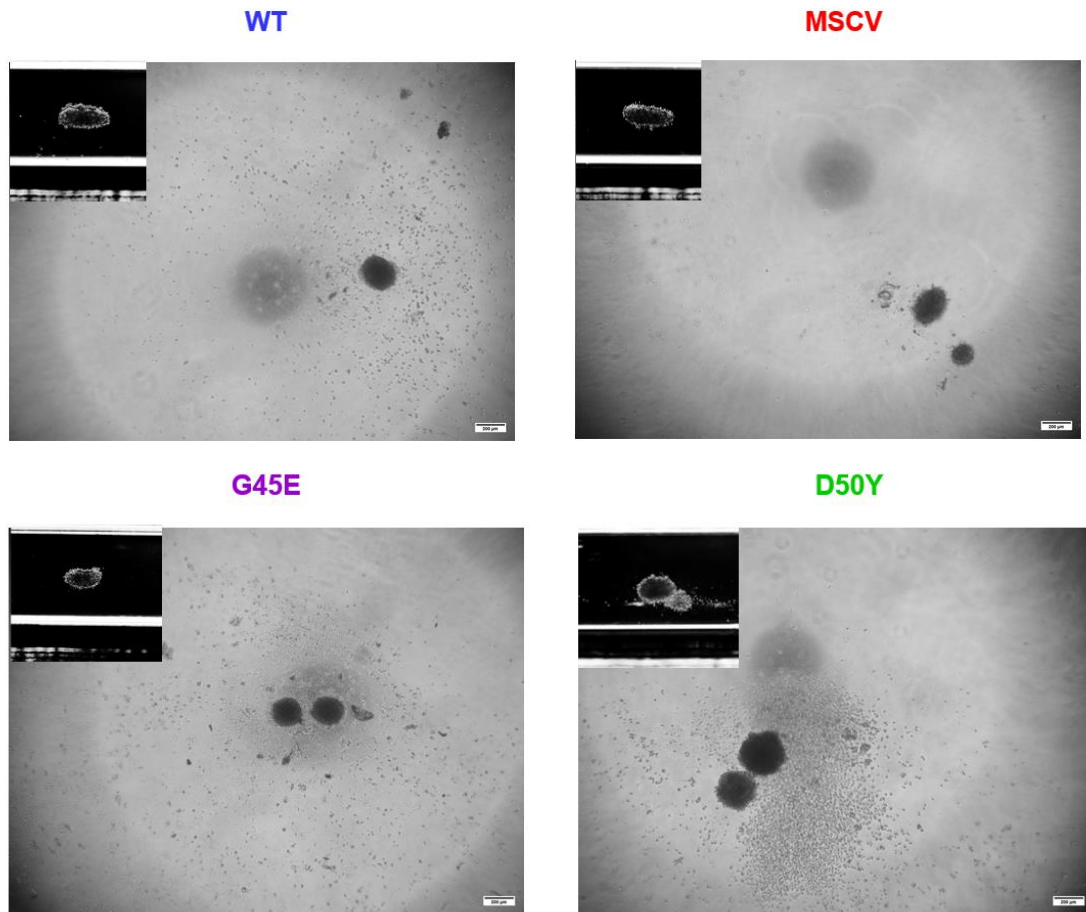
Figure 23. Images of cultures of four different HaCaT groups under magnetic levitation. Top left: Images of cells on day 0 within capillaries. Below, shown larger, are images taken on day 1 after each group was transferred onto agarose gels from the capillaries. Following this, the culture structures in the capillary obtained as a result of magnetic levitation culture were analyzed with the help of imageJ and the results were graphed according to the size parameters.

Afterwards, all cell groups; MSCV, WT, D50Y and G45E were cultured in magnetic levitation (Figure 22). At the end of this culture, they were transferred to agarose gel-embedded wells. It was observed that all cell groups maintained their more uniform structure when transferred to agarose after magnetic levitation. They formed a more uniform and unified spheroid structure than when transferred to agarose alone (Figure 23).

Eventually, the incorporation of magnetic levitation in addition to seeding cells onto agarose gel improved the observation of compact three-dimensional structures, rather than expecting uniform structures with agarose alone. Even in cultures using magnetic levitation alone, compact and well-formed 3D structures were observed within the capillaries. These structures maintained their integrity and structure when transferred from capillaries in the magnetic levitation system to agarose gel wells.

The size parameters were obtained by analyzing fluorescent microscope images during cell culture with magnetic levitation. The analysis illustrated (Figure 24) how each parameter corresponded to specific features of the cellular structures observed.
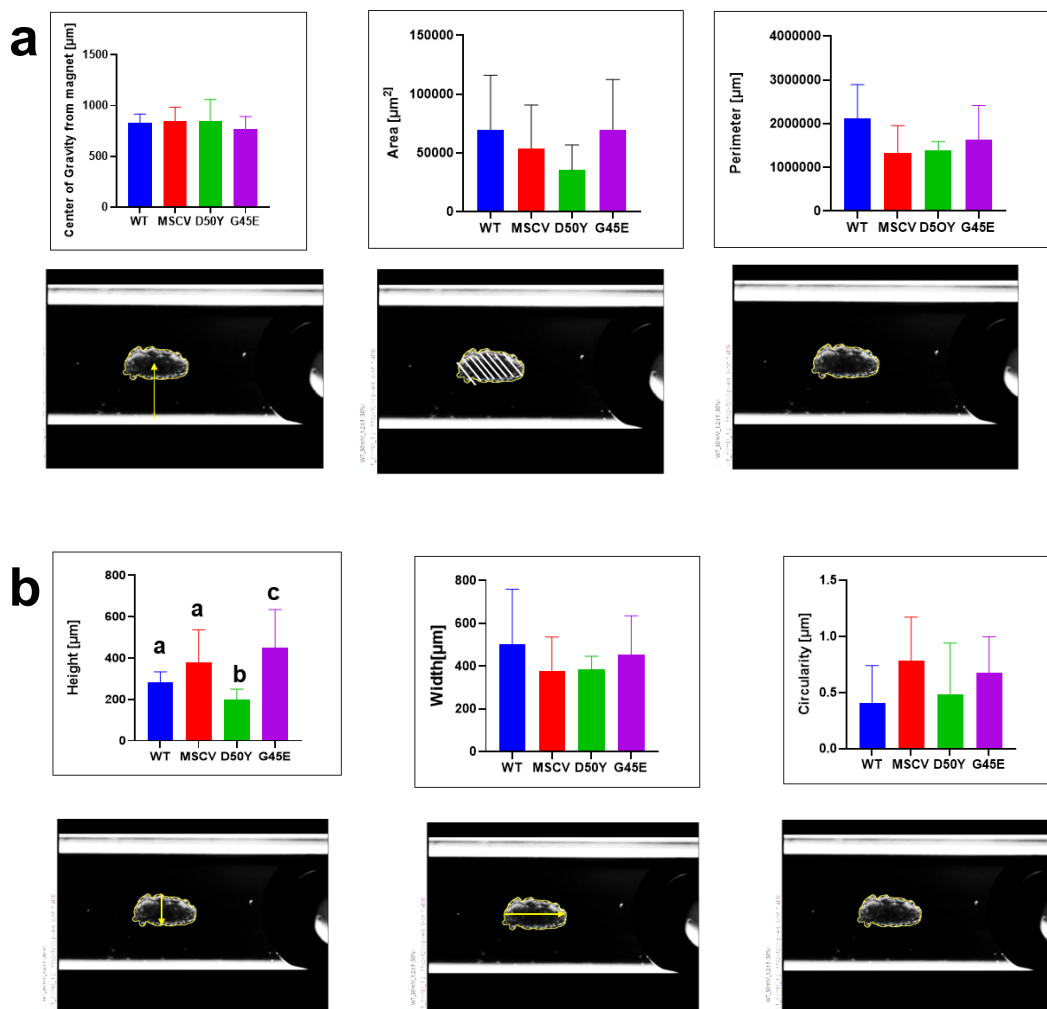
Figure 24. Demonstration and analysis of size parameters in different HaCaT cell groups. Parameters are as follows: a) from left to right center of gravity from magnet, area, perimeter; b) from left to right height, width, circularity.

Different size parameters, including area, perimeter, center of gravity, height, width, and circularity, were evaluated and tabulated. Descriptive statistics for these parameters were computed, and the results were presented in the following tables (Table 1, Table 2, Table 3, Table 4, Table 5, Table 6). This analysis provided insights into the overall distribution and characteristics of each parameter.

Table 1. Area parameter comparison of HaCaT groups, dimensional analysis.

Area (μm^2)				
	WT	**MSCV**	**D50Y**	**G45E**
Minimum	22078	15285	13282	21382
Median	64141	34819	31842	59345
Maximum	129007	129052	64084	216917
Range	106929	113766	50803	195535
Mean	69842	53779	35262	69622
Std. Deviation	46182	36950	21551	42872
Std. Error of Mean	23091	12317	10775	8102
Coefficient of variation	66.12%	68.71%	61.12%	61.58%
Skewness	0.598	1.127	0.8438	1.72
Kurtosis	-0.5141	0.7625	0.8612	3.97

Table 2. Perimeter parameter comparison of HaCaT groups, dimensional analysis.

Perimeter (µm)				
	WT	**MSCV**	**D50Y**	**G45E**
Minimum	1420655	699147	1106055	753207
Median	1966293	1077631	1434173	1502951
Maximum	3119838	2350255	1551559	4748483
Range	1699183	1651108	445504	3995276
Mean	2118270	1324215	1381490	1627620
Std. Deviation	769704	629042	207061	785020
Std. Error of Mean	384852	209681	103530	148355
Coefficient of variation	36.34%	47.50%	14.99%	48.23%
Skewness	0.8014	0.5547	-0.9608	2.483
Kurtosis	-1.09	-1.477	-0.6631	8.762

Table 3. Center of gravity parameter comparisons of the HaCaT groups, the dimensional analysis.

Center of Gravity (µm)				
	WT	**MSCV**	**D50Y**	**G45E**
Minimum	710.3	637.9	586.2	512.1
Median	841.4	844.8	874.1	767.2
Maximum	917.2	1124	1048	1059
Range	206.9	486.2	462.1	546.6
Mean	827.6	843.9	845.7	766.9
Std. Deviation	88.86	141.1	214.7	126.5
Std. Error of Mean	44.43	47.04	107.4	23.91
Coefficient of variation	10.74%	16.72%	25.39%	16.50%
Skewness	-0.7818	0.6576	-0.451	0.2809
Kurtosis	0.2168	1.083	-2.901	0.1524

Table 4. Height parameter comparison of HaCaT groups, dimensional analysis.

Height (µm)				
	WT	**MSCV**	**D50Y**	**G45E**
Minimum	237.9	208.6	150	217.2
Median	280.2	320.7	199.1	427.6
Maximum	339.7	591.4	250	1145
Range	101.7	382.8	100	927.6
Mean	284.5	378.5	199.6	452
Std. Deviation	49.27	157.5	50	183.1
Std. Error of Mean	24.64	52.49	25	34.6
Coefficient of variation	17.32%	41.60%	25.05%	40.51%
Skewness	0.2262	0.1832	0.01725	1.931
Kurtosis	-4.304	-2.134	-5.163	6.626

Table 5. Width parameter comparison of HaCaT groups, dimensional analysis.

Width (µm)				
	WT	**MSCV**	**D50Y**	**G45E**
Minimum	256.9	208.6	306.9	217.2
Median	444.8	320.7	395.7	427.6
Maximum	862.1	591.4	448.3	1145
Range	605.2	382.8	141.4	927.6
Mean	502.2	378.5	386.6	452
Std. Deviation	257.6	157.5	59.6	183.1
Std. Error of Mean	128.8	52.49	29.8	34.6
Coefficient of variation	51.31%	41.60%	15.41%	40.51%
Skewness	1.208	0.1832	-0.826	1.931
Kurtosis	1.994	-2.134	1.057	6.626

Table 6. Circularity parameter comparison of HaCaT groups, dimensional analysis.

Circularity (µm)				
	WT	**MSCV**	**D50Y**	**G45E**
Minimum	0.08966	0.1362	0.1224	0.09828
Median	0.3405	0.8	0.344	0.6629
Maximum	0.8672	1.371	1.134	1.2
Range	0.7776	1.234	1.012	1.102
Mean	0.4095	0.781	0.4862	0.6727
Std. Deviation	0.3301	0.3893	0.4527	0.3239
Std. Error of Mean	0.165	0.1298	0.2264	0.06122
Coefficient of variation	80.61%	49.85%	93.11%	48.15%
Skewness	1.138	-0.1125	1.504	-0.0389
Kurtosis	1.827	-0.4945	2.2	-1.029

Upon examining the area values, the average measurements were as follows: 69842 µm² for WT, 53779 µm² for MSCV, 35262 µm² for D50Y, and 69622 µm² for G45E; In terms of mean area values, D50Y exhibited smaller values compared to the other groups. The standard deviations for WT, MSCV, D50Y, and G45E were 46182, 36950, 21551, and 42872, respectively. Skewness values were also calculated, showing 0.598 for WT, 1.127 for MSCV, 0.8438 for D50Y, and 1.72 for G45E (Table 1).

When examining the perimeter values, the average measurements were: 2118270 µm for WT, 1324215 µm for MSCV, 1381490 µm for D50Y, and 1627620 µm for G45E. The standard deviations were 769704 µm for WT, 629042 µm for MSCV, 207061 µm for D50Y, and 785020 µm for G45E. The skewness values were 0.8014 for WT, 0.5547 for MSCV, -0.9608 for D50Y, and 2.483 for G45E (Table 2).

The average measurements for the center of gravity: WT: 827,6 µm, MSCV: 843,9 µm, D50Y: 845,7 µm and G45E: 766.9 µm. Standard deviations were 88.86 for WT, 141.1 for MSCV, 214.7 for D50Y and 126.5 for G45E. Here the G45E average value turned out to be slightly smaller. For the center of gravity, the skewness was as follows: -0.7818 for WT, 0.6576 for MSCV, -0.451 for D50Y, and 0.2809 for G45E (Table 3).

When examining the height (μm) values, the average measurements were; WT: 284.5 μm, MSCV: 378.5 μm, D50Y: 199.6 μm, and G45E: 452 μm. The standard deviations were 49.27 μm for WT, 157.5 μm for MSCV, 50 μm for D50Y, and 183.1 μm for G45E. The skewness values were 0.2262 for WT, 0.1832 for MSCV, 0.01725 for D50Y, and 1.931 for G45E (Table 4).

When examining the width (μm) values, the average measurements were: WT: 502.2 μm, MSCV: 378.5 μm, D50Y: 386.6 μm, and G45E: 452 μm. The standard deviations were 257.6 μm for WT, 157.5 μm for MSCV, 59.6 μm for D50Y, and 183.1 μm for G45E. The skewness values were 1.208 for WT, 0.1832 for MSCV, -0.826 for D50Y, and 1.931 for G45E. (Table 5).

As can be seen in the figures, the shapes of the formed structures were mostly elliptical, not much round-like shapes were observed, therefore circularity values were as follows Upon examining the circularity values, the average measurements were: WT: 0.4095 μm, MSCV: 0.781 μm, D50Y: 0.4862 μm, and G45E: 0.6727 μm. The standard deviations for WT, MSCV, D50Y, and G45E were 0.3301, 0.3893, 0.4527, and 0.3239, respectively. The skewness values were 1.138 for WT, -0.1125 for MSCV, 1.504 for D50Y, and -0.03888 for G45E (Table 6).

The magnetic levitation culture method showed significant advantages in maintaining the homogeneity and structural integrity of cell groups when transferred to agarose. Spheroid structures formed after levitation were significantly more coherent and consistent than those transferred directly to agarose. This homogeneity is critical to ensure reproducibility and reliability in tissue engineering applications. Generally, the size parameters showed similar results in all groups (Figure 24). Furthermore, when comparing the four groups (MSCV, WT, D50Y, G45E), the significant height difference in the G45E group at certain Gd^{3+} concentrations highlight the importance of fine-tuning experimental conditions for optimal results. These findings confirm the standardization and reproducibility of our method and highlight its potential as a practical alternative for future research and applications in skin tissue engineering.

CHAPTER 4

CONCLUSION

The aim of this study was to develop precise methods to measure keratinocyte density at the single cell level and to investigate how variations in single cell density affect keratinocyte behavior and function. Furthermore, using MagLev technology, we aim to provide an alternative to the creation of 3D keratinocyte constructs by assessing their structural integrity and functionality for tissue engineering.

Our initial expectations were to observe clear differences between mutated HaCaT cells and control groups. Through optimization experiments using the MSCV vector, we found that the Gd^{3+} concentrations of 15 mM and 30 mM were suitable for further experiments with other HaCaT groups. Single cell density measurements revealed significant differences, especially in the G45E group at 15 mM, as confirmed by Tukey test, whereas at 30 mM the comparison between MSCV and G45E showed no significant difference. These results led us to plan further experiments with a concentration of 15 mM. standardization and reproducibility for HaCaT cells were demonstrated throughout the study. The obtained levitation data were calibrated, and densities were obtained; keratinocytes were analyzed according to single cell density for the first time. Previous magnetic levitation studies have determined the density of various cell types including cancer cells (1.044-1.084 g/ml) (Durmuş et al., 2015), bone marrow cells (1.07 g/ml) (Sarıgil et al., 2019), adipocytes (0.989 g/ml) (Sarıgil et al., 2020), white blood cells (1.088 g/ml) and red blood cells (1.109 g/ml) (Durmuş et al., 2015). Keratinocytes generally showed a high density around 1.091 g/ml when compared to these other cell types. However, the G45E group showed a lower density. This difference in density may serve as an indicator to distinguish this specific condition. The findings have improved the understanding of the biophysical properties of keratinocytes.

In biofabrication experiments, it was determined that a concentration of 30 mM Gd^{3+} was the optimal value to prevent cell adhesion to capillary walls. Although size

parameters were similar between groups, a significant height difference was noted in the G45E group, further confirming the standardization and reproducibility of our experimental approach. In experiments involving transfer of magnetic levitation culture to agarose, they formed a more coherent and consistent spheroid structure compared to those previously transferred to agarose without magnetic levitation. Because when cells were seeded directly on agarose gel using only gold standard, disorganized and discrete structures were formed. On the other hand, keratinocyte structures maintained their structural integrity when supported by magnetic levitation technique and facilitated transfer for further 3D culture.

In conclusion, this study successfully demonstrated reproducible and scaffold-free biofabrication of living keratinocyte cell constructs using magnetic levitation. These results improve the understanding of the biophysical properties of keratinocytes and suggest that label-free, scaffold-free magnetic levitation may be a practical alternative for future applications in tissue engineering. Therefore, this innovative approach holds promise for the advancement of tissue engineering and regenerative medicine by providing a reliable method to create complex tissue constructs without the need for conventional scaffold materials.

REFERENCES

Aleemardani, Mina, Michael Augustine, Robin. 2018. "Skin Bioprinting: A Novel Approach for Creating Artificial Skin From Synthetic and Natural Building Blocks." *Progress in Biomaterials* 7 (2): 77–92. https://doi.org/10.1007/s40204-018-0087-0.

Anil-Inevi, Muge, Kerem Delikoyun, Gulistan Mese, Hüseyin C. Tekin, and Engin Ozcivici. 2021. "Magnetic Levitation Assisted Biofabrication, Culture, and Manipulation of 3D Cellular Structures Using a Ring Magnet Based Setup." *Biotechnology and Bioengineering* 118 (12): 4771–85. https://doi.org/10.1002/bit.27941.

Anil-Inevi, Muge, Sena Yaman, Ahu Arslan Yildiz, Gulistan Mese, Ozden Yalcin-Ozuysal, Hüseyin C. Tekin, and Engin Ozcivici. 2018. "Biofabrication of in Situ Self Assembled 3D Cell Cultures in a Weightlessness Environment Generated Using Magnetic Levitation." *Scientific Reports* 8 (1): 7239. https://doi.org/10.1038/s41598-018-25718-9.

Ashkarran, Ali Akbar, and Morteza Mahmoudi. 2021. "Magnetic Levitation Systems for Disease Diagnostics." *Trends in Biotechnology* 39 (3): 311–21. https://doi.org/10.1016/j.tibtech.2020.07.010.

Baday, Murat, Semih Calamak, Naside Gozde Durmus, Ronald W. Davis, Lars M. Steinmetz, and Utkan Demirci. 2015. "Integrating Cell Phone Imaging With Magnetic Levitation (i-LEV) for Label-Free Blood Analysis at the Point-of-Living." *Small* 12 (9): 1222–29. https://doi.org/10.1002/smll.201501845.

Bakondi, Edina, Mónika Gönczi, Éva Szabó, Péter Bai, Pál Pacher, Pál Gergely, László Kovács, et al. 2003. "Role of Intracellular Calcium Mobilization and Cell-Density-Dependent Signaling in Oxidative-Stress-Induced Cytotoxicity in HaCaT Keratinocytes." *Journal of Investigative Dermatology* 121 (1): 88–95. https://doi.org/10.1046/j.1523-1747.2003.12329.x.

Bannasch, Holger, Matthias Föhn, Tim Unterberg, Alexander D Bach, Birgit Weyand, and G Björn Stark. 2003. "Skin Tissue Engineering." *Clinics in Plastic Surgery* 30 (4): 573–79. https://doi.org/10.1016/s0094-1298(03)00075-0.

Barros, Natan R, Han-Jun Kim, Marcus J Gouidie, KangJu Lee, Praveen Bandaru, Ethan A Banton, Einollah Sarikhani, et al. 2021. "Biofabrication of Endothelial Cell, Dermal Fibroblast, and Multilayered Keratinocyte Layers for Skin Tissue Engineering." *Biofabrication* 13 (3): 035030. https://doi.org/10.1088/1758-5090/aba503.

Baumbauer, Kyle M, Jennifer J DeBerry, Peter C Adelman, Richard H Miller, Junichi Hachisuka, Kuan Hsien Lee, Sarah E Ross, Richard H Koerber, Brian M Davis, and Kathryn M Albers. 2015. "Keratinocytes Can Modulate and Directly Initiate Nociceptive Responses." *eLife* 4 (9): e09674. https://doi.org/10.7554/elife.09674.

Berthiaume, François, Timothy J. Maguire, and Martin L. Yarmush. 2011. "Tissue Engineering and Regenerative Medicine: History, Progress, and Challenges." *Annual Review of Chemical and Biomolecular Engineering* 2 (1): 403–30. https://doi.org/10.1146/annurev-chembioeng-061010-114257.

Bikle, Daniel D., Yan Jiang, Thai Nguyen, Yuko Oda, and Chia-Ling Tu. 2016. "Disruption of Vitamin D and Calcium Signaling in Keratinocytes Predisposes to Skin Cancer." *Frontiers in Physiology* 7 (7): 296. https://doi.org/10.3389/fphys.2016.00296.

Breitkreutz, Dirk, Hans-Jürgen Stark, Peter Plein, Markus Baur, and Norbert E. Fusenig. 1993. "Differential Modulation of Epidermal Keratinization in Immortalized (HaCaT) and Tumorigenic Human Skin Keratinocytes (HaCaT-ras) by Retinoic Acid and Extracellular Ca2+." *Differentiation* 54 (3): 201–17. https://doi.org/10.1111/j.1432-0436.1993.tb01602.x.

Burns, Tony., Breathnach, Stephen, Cox, Neil., & Griffiths, Christopher. (Eds.). (2010). *Rook's Textbook of Dermatology*. Wiley. https://doi.org/10.1002/9781444317633

Cancedda, Ranieri, Beatrice Dozin, Paolo Giannoni, and Rodolfo Quarto. 2003. "Tissue Engineering and Cell Therapy of Cartilage and Bone." *Matrix Biology* 22 (1): 81–91. https://doi.org/10.1016/s0945-053x(03)00012-x.

Castro, Nicolas., Stephan. Ribeiro, Miguel. M. Fernandes, Clarisse. Ribeiro, Vitor. Cardoso, Valdelice. Correia, Roberto. Minguez, and S. Lanceros-Mendez. 2020. "Physically Active Bioreactors for Tissue Engineering Applications." *Advanced Biosystems* 4 (10): e2000125. https://doi.org/10.1002/adbi.202000125.

Chakraborty, Juhi, Shikha Chawla, and Sourabh Ghosh. 2022. "Developmental Biology-inspired Tissue Engineering by Combining Organoids and 3D Bioprinting." *Current Opinion in Biotechnology* 78 (12): 102832. https://doi.org/10.1016/j.copbio.2022.102832.

Chandra, Prafulla K., Shay Soker, and Anthony Atala. 2020. "Tissue Engineering: Current Status and Future Perspectives." In *Elsevier eBooks*, 1–35. https://doi.org/10.1016/b978-0-12-818422-6.00004-6.

Chattopadhyay, Pratip K, Todd M Gierahn, Mario Roederer, and J Christopher Love. 2014. "Single-cell Technologies for Monitoring Immune Systems." *Nature Immunology* 15 (2): 128–35. https://doi.org/10.1038/ni.2796.

Chaudhari, Atul, Komal Vig, Dieudonné Baganizi, Rajnish Sahu, Saurabh Dixit, Vida Dennis, Shree Singh, and Shreekumar Pillai. 2016. "Future Prospects for Scaffolding Methods and Biomaterials in Skin Tissue Engineering: A Review." *International Journal of Molecular Sciences* 17 (12): 1974. https://doi.org/10.3390/ijms17121974.

Chhabra, Preeti, David E.R. Sutherland, and Kenneth L. Brayman. 2014. "Overcoming Barriers in Clinical Islet Transplantation: Current Limitations and Future Prospects." *Current Problems in Surgery* 51 (2): 49–86. https://doi.org/10.1067/j.cpsurg.2013.10.002.

Choi, Moonju, and Choongho Lee. 2015. "Immortalization of Primary Keratinocytes and Its Application to Skin Research." *Biomolecules & Therapeutics* 23 (5): 391–99. https://doi.org/10.4062/biomolther.2015.038.

Crucianelli, Laura, and H. Henrik Ehrsson. 2022. "The Role of the Skin in Interoception: A Neglected Organ?" *Perspectives on Psychological Science* 18 (1): 224–38. https://doi.org/10.1177/17456916221094509.

Dabbagh, Sajjad Rahmani, M. Munzer Alseed, Milad Saadat, Metin Sitti, and Savas Tasoglu. 2021. "Biomedical Applications of Magnetic Levitation." *Advanced NanoBiomed Research* 2 (3): 2100103 https://doi.org/10.1002/anbr.202100103.

Dai, Christina, Shawn Shih, and Amor Khachemoune. 2020. "Skin Substitutes for Acute and Chronic Wound Healing: An Updated Review." *Journal of Dermatological Treatment* 31 (6): 639–48. https://doi.org/10.1080/09546634.2018.1530443.

Daquinag, Alexes C., Glauco R. Souza, and Mikhail G. Kolonin. 2013. "Adipose Tissue Engineering in Three-Dimensional Levitation Tissue Culture System Based on Magnetic Nanoparticles." *Tissue Engineering Part C Methods* 19 (5): 336–44. https://doi.org/10.1089/ten.tec.2012.0198.

Da Silveira Dos Santos, Aline Xavier, and Prisca Liberali. 2018. "From Single Cells to Tissue Self-organization." *FEBS Journal* 286 (8): 1495–1513. https://doi.org/10.1111/febs.14694.

De Vargas Roditi, Laura, and Manfred Claassen. 2015. "Computational and Experimental Single Cell Biology Techniques for the Definition of Cell Type Heterogeneity, Interplay and Intracellular Dynamics." *Current Opinion in Biotechnology* 34 (8): 9–15. https://doi.org/10.1016/j.copbio.2014.10.010.

Dixit, Saurabh, Dieudonné R. Baganizi, Rajnish Sahu, Ejowke Dosunmu, Atul Chaudhari, Komal Vig, Shreekumar R. Pillai, Shree R. Singh, and Vida A. Dennis. 2017. "Immunological Challenges Associated With Artificial Skin Grafts: Available Solutions and Stem Cells in Future Design of Synthetic Skin." *Journal of Biological Engineering* 11 (1): 49. https://doi.org/10.1186/s13036-017-0089-9.

Durmus, Naside Gozde, H. Cumhur Tekin, Sinan Guven, Kaushik Sridhar, Ahu Arslan Yildiz, Gizem Calibasi, Ionita Ghiran, Ronald W. Davis, Lars M. Steinmetz, and Utkan Demirci. 2015a. "Magnetic Levitation of Single Cells." *Proceedings of the National Academy of Sciences* 112 (28): e3661-e3668 https://doi.org/10.1073/pnas.1509250112.

Eckert, Rebecca. L., John. F. Crish, and Nate. A. Robinson. 1997. "The Epidermal Keratinocyte as a Model for the Study of Gene Regulation and Cell Differentiation." *Physiological Reviews* 77 (2): 397–424. https://doi.org/10.1152/physrev.1997.77.2.397.

Elias, Peter M., Kenneth R. Feingold, Mathew J. Hardman, and Carolyn Byrne. 2005. "Skin Structural Development." In *Skin Barrier*, 1st Edition, 16. CRC Press. ISBN 9780429163470

Gerido, Dwan A, Adam M DeRosa, Gabriele Richard, and Thomas W White. 2007. "Aberrant Hemichannel Properties of Cx26 Mutations Causing Skin Disease and Deafness." *AJP Cell Physiology* 293 (1): 337–45. https://doi.org/10.1152/ajpcell.00626.2006.

Gilpin, Anna, and Yong Yang. 2017. "Decellularization Strategies for Regenerative Medicine: From Processing Techniques to Applications." *BioMed Research International* 2017 (1): 1–13. https://doi.org/10.1155/2017/9831534.

Gomer, Richard H., Wonhee Jang, and Derrick Brazill. 2011. "Cell Density Sensing and Size Determination." *Development Growth & Differentiation* 53 (4): 482–94. https://doi.org/10.1111/j.1440-169x.2010.01248.x.

Goranov, V., T. Shelyakova, R. De Santis, Y. Haranava, A. Makhaniok, A. Gloria, A. Tampieri, et al. 2020. "3D Patterning of Cells in Magnetic Scaffolds for Tissue Engineering." *Scientific Reports* 10 (1): 2289. https://doi.org/10.1038/s41598-020-58738-5.

Green, Barry G. 2004. "Temperature Perception and Nociception." *Journal of Neurobiology* 61 (1): 13–29. https://doi.org/10.1002/neu.20081.

Greenspan, Joel D., and Stanley J. Bolanowski. 1996. "The Psychophysics of Tactile Perception and Its Peripheral Physiological Basis." In *Elsevier eBooks*, 25–103. https://doi.org/10.1016/b978-012426910-1/50004-2.

Grover, William H., Andrea K. Bryan, Monica Diez-Silva, Subra Suresh, John M. Higgins, and Scott R. Manalis. 2011. "Measuring Single-cell Density." *Proceedings of the National Academy of Sciences* 108 (27): 10992–96. https://doi.org/10.1073/pnas.1104651108.

Gschwandtner, M., Mark. Mildner, Volger. Mlitz, Florian. Gruber, Leopold. Eckhart, Thomas. Werfel, R. Gutzmer, P. M. Elias, and E. Tschachler. 2012. "Histamine Suppresses Epidermal Keratinocyte Differentiation and Impairs Skin Barrier Function in a Human Skin Model." *Allergy* 68 (1): 37–47. https://doi.org/10.1111/all.12051.

Guo, Bang J., Zhen L. Yang, and Long J. Zhang. 2018. "Gadolinium Deposition in Brain: Current Scientific Evidence and Future Perspectives." *Frontiers in Molecular Neuroscience* 11 (9): 335. https://doi.org/10.3389/fnmol.2018.00335.

Hu, Huiqian, L. Krishaa, and Eliza Li Shan Fong. 2023a. "Magnetic Force-based Cell Manipulation for in Vitro Tissue Engineering." *APL Bioengineering* 7 (3): 049901. https://doi.org/10.1063/5.0138732.

Jackson, Hartland W., Jana R. Fischer, Vito R. T. Zanotelli, H. Raza Ali, Robert Mechera, Savas D. Soysal, Holger Moch, et al. 2020. "The Single-cell Pathology Landscape

of Breast Cancer." *Nature* 578 (7796): 615–20. https://doi.org/10.1038/s41586-019-1876-x.

Jepps, Owen G., Yuri Dancik, Yuri G. Anissimov, and Michael S. Roberts. 2013. "Modeling the Human Skin Barrier — Towards a Better Understanding of Dermal Absorption." *Advanced Drug Delivery Reviews* 65 (2): 152–68. https://doi.org/10.1016/j.addr.2012.04.003.

Jung, Taek-Hee, Eun-Bin Chung, Hyung Woo Kim, Seong Woo Choi, Soon-Jung Park, Anthony Safaa Mukhtar, Hyung-Min Chung, et al. 2020. "Application of Co-culture Technology of Epithelial Type Cells and Mesenchymal Type Cells Using Nanopatterned Structures." *PLoS ONE* 15 (5): e0232899. https://doi.org/10.1371/journal.pone.0232899.

Kecili, Seren, Esra Yilmaz, Ozge Solmaz Ozcelik, Muge Anil-Inevi, Zehra Elif Gunyuz, Ozden Yalcin-Ozuysal, Engin Ozcivici, and H. Cumhur Tekin. 2023. "µDACS Platform: A Hybrid Microfluidic Platform Using Magnetic Levitation Technique and Integrating Magnetic, Gravitational, and Drag Forces for Density-based Rare Cancer Cell Sorting." *Biosensors and Bioelectronics X* 15 (12): 100392. https://doi.org/10.1016/j.biosx.2023.100392.

Kianian, Sara, Kelley Zhao, Jasleen Kaur, Kimberly W. Lu, Sourish Rathi, Kanad Ghosh, Hunter Rogoff, et al. 2023. "Autologous Skin Grafts, Versus Tissue-engineered Skin Constructs: A Systematic Review and Meta-analysis." *Plastic & Reconstructive Surgery Global Open* 11 (6): e5100. https://doi.org/10.1097/gox.0000000000005100.

Kirfel, Gregor., and Verena. Herzog. 2004. "Migration of Epidermal Keratinocytes: Mechanisms, Regulation, and Biological Significance." *PROTOPLASMA* 223 (2–4): 67-78. https://doi.org/10.1007/s00709-003-0031-5.

Kolarsick, Paul a. J., Maria Ann Kolarsick, and Carolyn Goodwin. 2011. "Anatomy and Physiology of the Skin." *Journal of the Dermatology Nurses' Association* 3 (4): 203–13. https://doi.org/10.1097/jdn.0b013e3182274a98.

Krishnaswamy, Smita, Matthew H. Spitzer, Michael Mingueneau, Sean C. Bendall, Oren Litvin, Erica Stone, Dana Pe'er, and Garry P. Nolan. 2014. "Conditional Density-based Analysis of T Cell Signaling in Single-cell Data." *Science* 346 (6213): 1250689. https://doi.org/10.1126/science.1250689.

Lanza, Robert, Robert Langer, Joseph P. Vacanti, and Anthony Atala. 2020. *Principles of Tissue Engineering*. Academic Press.

Lee, Eung-Ryoung, Yong-Jin Kang, Jung-Hyun Kim, Hoon Taek Lee, and Ssang-Goo Cho. 2005. "Modulation of Apoptosis in HaCaT Keratinocytes via Differential Regulation of ERK Signaling Pathway by Flavonoids." *Journal of Biological Chemistry* 280 (36): 31498–507. https://doi.org/10.1074/jbc.m505537200.

Lehmann, Bodo, Kerstin Querings, and Jörg Reichrath. 2004. "Vitamin D and Skin: New Aspects for Dermatology." *Experimental Dermatology* 13 (4): 11–15. https://doi.org/10.1111/j.1600-0625.2004.00257.x.

Longo, Sophia K., Margaret G. Guo, Andrew L. Ji, and Paul A. Khavari. 2021. "Integrating Single-cell and Spatial Transcriptomics to Elucidate Intercellular Tissue Dynamics." *Nature Reviews Genetics* 22 (10): 627–44. https://doi.org/10.1038/s41576-021-00370-8.

Lumpkin, Ellen A., and Michael J. Caterina. 2007. "Mechanisms of Sensory Transduction in the Skin." *Nature* 445 (7130): 858–65. https://doi.org/10.1038/nature05662.

Lyu, Chenxin, Chengqian Zhang, Daofan Tang, and Peng Zhao. 2024a. "Magnetic Levitation in Medicine and Bioengineering." In *Magnetic Levitation*, 163–79. https://doi.org/10.1007/978-981-99-8314-8_9.

Markiewicz-Gospodarek, Agnieszka, Małgorzata Kozioł, Maciej Tobiasz, Jacek Baj, Elżbieta Radzikowska-Büchner, and Agata Przekora. 2022. "Burn Wound Healing: Clinical Complications, Medical Care, Treatment, and Dressing Types: The Current State of Knowledge for Clinical Practice." *International Journal of Environmental Research and Public Health* 19 (3): 1338. https://doi.org/10.3390/ijerph19031338.

Mathes, Stephanie H., Heinz Ruffner, and Ursula Graf-Hausner. 2014. "The Use of Skin Models in Drug Development." *Advanced Drug Delivery Reviews* 69–70 (4): 81–102. https://doi.org/10.1016/j.addr.2013.12.006.

Mathys, Hansruedi, Jose Davila-Velderrain, Zhuyu Peng, Fan Gao, Shahin Mohammadi, Jennie Z. Young, Madhvi Menon, et al. 2019. "Single-cell Transcriptomic Analysis of Alzheimer's Disease." *Nature* 570 (7761): 332–37. https://doi.org/10.1038/s41586-019-1195-2.

Mendibil, Unai, Raquel Ruiz-Hernandez, Sugoi Retegi-Carrion, Nerea Garcia-Urquia, Beatriz Olalde-Graells, and Ander Abarrategi. 2020. "Tissue-Specific Decellularization Methods: Rationale and Strategies to Achieve Regenerative Compounds." *International Journal of Molecular Sciences* 21 (15): 5447. https://doi.org/10.3390/ijms21155447.

Moran, Mary C., Radha P. Pandya, Kimberly A. Leffler, Takeshi Yoshida, Lisa A. Beck, and Matthew G. Brewer. 2021. "Characterization of Human Keratinocyte Cell Lines for Barrier Studies." *JID Innovations* 1 (2): 100018. https://doi.org/10.1016/j.xjidi.2021.100018.

Munaz, Ahmed, Muhammad J. A. Shiddiky, and Nam-Trung Nguyen. 2018. "Recent Advances and Current Challenges in Magnetophoresis Based Micro Magnetofluidics." *Biomicrofluidics* 12 (3): 031501. https://doi.org/10.1063/1.5035388.

Niehues, Hanna, Joke A. Bouwstra, Abdoelwaheb El Ghalbzouri, Johanna M. Brandner, Patrick L. J. M. Zeeuwen, and Ellen H. Van Den Bogaard. 2018. "3D Skin Models for 3R Research: The Potential of 3D Reconstructed Skin Models to Study Skin Barrier Function." *Experimental Dermatology* 27 (5): 501–11. https://doi.org/10.1111/exd.13531.

Parfenov, Vladislav A, Stanislav V Petrov, Frederico D a S Pereira, Aleksandr A Levin, Elizaveta V Koudan, Elizaveta K Nezhurina, Pavel A Karalkin, et al. 2020. "Scaffold-free, Label-free, and Nozzle-free Magnetic Levitational Bioassembler for Rapid Formative Biofabrication of 3D Tissues and Organs." *International Journal of Bioprinting* 6 (3): 110–19. https://doi.org/10.18063/ijb.v6i3.304.

Pars, Selin, Kevin Achberger, Alexander Kleger, Stefan Liebau, and Natalia Pashkovskaia. 2021. "Generation of Functional Vascular Endothelial Cells and Pericytes From Keratinocyte Derived Human Induced Pluripotent Stem Cells." *Cells* 10 (1): 74. https://doi.org/10.3390/cells10010074.

Piipponen, Minna, Dongqing Li, and Ning Xu Landén. 2020. "The Immune Functions of Keratinocytes in Skin Wound Healing." *International Journal of Molecular Sciences* 21 (22): 8790. https://doi.org/10.3390/ijms21228790.

Piotrowska, Anna, Justyna Wierzbicka, and Michał A Żmijewski. 2016. "Vitamin D in the Skin Physiology and Pathology." *Acta Biochimica Polonica* 63 (1): 17-29. https://doi.org/10.18388/abp.2015_1104.

Pourzand, Charareh, Andrea Albieri-Borges, and Nico N. Raczek. 2022. "Shedding a New Light on Skin Aging, Iron- and Redox-Homeostasis and Emerging Natural Antioxidants." *Antioxidants* 11 (3): 471. https://doi.org/10.3390/antiox11030471

Proksch, Ehrhardt, Johanna M. Brandner, and Jens-Michael Jensen. 2008. "The Skin: An Indispensable Barrier." *Experimental Dermatology* 17 (12): 1063–72. https://doi.org/10.1111/j.1600-0625.2008.00786.x.

Quan, Taihao, Frank Wang, Yuan Shao, Laure Rittié, Wei Xia, Jeffrey S. Orringer, John J. Voorhees, and Gary J. Fisher. 2013. "Enhancing Structural Support of the Dermal Microenvironment Activates Fibroblasts, Endothelial Cells, and Keratinocytes in Aged Human Skin in Vivo." *Journal of Investigative Dermatology* 133 (3): 658–67. https://doi.org/10.1038/jid.2012.364.

Ramms, Lena, Gloria Fabris, Reinhard Windoffer, Nicole Schwarz, Ronald Springer, Chen Zhou, Jaroslav Lazar, et al. 2013. "Keratins as the Main Component for the Mechanical Integrity of Keratinocytes." *Proceedings of the National Academy of Sciences* 110 (46): 18513–18. https://doi.org/10.1073/pnas.1313491110.

Ratushny, Vladimir, Michael D. Gober, Ryan Hick, Todd W. Ridky, and John T. Seykora. 2012. "From Keratinocyte to Cancer: The Pathogenesis and Modeling of Cutaneous Squamous Cell Carcinoma." *Journal of Clinical Investigation* 122 (2): 464–72. https://doi.org/10.1172/jci57415.

Rinn, John L., Jordon K. Wang, Helen Liu, Kelli Montgomery, Matt Van De Rijn, and Howard Y. Chang. 2008. "A Systems Biology Approach to Anatomic Diversity of Skin." *Journal of Investigative Dermatology* 128 (4): 776–82. https://doi.org/10.1038/sj.jid.5700986.

Rijal, Girdhari, and Weimin Li. 2018. "Native-mimicking in Vitro Microenvironment: An Elusive and Seductive Future for Tumor Modeling and Tissue Engineering." *Journal of Biological Engineering* 12 (1): 20. https://doi.org/10.1186/s13036-018-0114-7.

Roberts, Michael, Mark Pellett, and Sheree Elizabeth Cross. 2002. "Skin Transport." In *Drugs and the Pharmaceutical Sciences*, 88–194. https://doi.org/10.1201/9780824743239.ch4.

Rogosnitzky, Moshe, and Stacy Branch. 2016. "Gadolinium-based Contrast Agent Toxicity: A Review of Known and Proposed Mechanisms." *BioMetals* 29 (3): 365–76. https://doi.org/10.1007/s10534-016-9931-7.

Russo, Barbara, Nicolò C. Brembilla, and Carlo Chizzolini. 2020. "Interplay Between Keratinocytes and Fibroblasts: A Systematic Review Providing a New Angle for Understanding Skin Fibrotic Disorders." *Frontiers in Immunology* 11 (3): 648. https://doi.org/10.3389/fimmu.2020.00648.

Salgado, António J., Joaquim M. Oliveira, Albino Martins, Fábio G. Teixeira, Nuno A. Silva, Nuno M. Neves, Nuno Sousa, and Rui L. Reis. 2013. "Tissue Engineering

and Regenerative Medicine." *International Review of Neurobiology*, (1), 1–33. https://doi.org/10.1016/b978-0-12-410499-0.00001-0.

Sarigil, Oyku, Muge Anil-Inevi, Esra Yilmaz, Gulistan Mese, H. Cumhur Tekin, and Engin Ozcivici. 2019. "Label-free Density-based Detection of Adipocytes of Bone Marrow Origin Using Magnetic Levitation." *The Analyst* 144 (9): 2942–53. https://doi.org/10.1039/c8an02503g.

Schuerle, Simone, Sandro Erni, Marten. Flink, Bradley.E. Kratochvil, and Bradley.J. Nelson. 2013. "Three-Dimensional Magnetic Manipulation of Micro- and Nanostructures for Applications in Life Sciences." *IEEE Transactions on Magnetics* 49 (1): 321–30. https://doi.org/10.1109/tmag.2012.2224693.

Shevchenko, Rostislav V., Stuart L. James, and S. Elizabeth James. 2009. "A Review of Tissue-engineered Skin Bioconstructs Available for Skin Reconstruction." *Journal of the Royal Society Interface* 7 (43): 229–58. https://doi.org/10.1098/rsif.2009.0403.

Shuja, Zunaira, Leping Li, Shashank Gupta, Gülistan Meşe, and Thomas W. White. 2016. "Connexin26 Mutations Causing Palmoplantar Keratoderma and Deafness Interact With Connexin43, Modifying Gap Junction and Hemichannel Properties." *Journal of Investigative Dermatology* 136 (1): 225–35. https://doi.org/10.1038/jid.2015.389.

Silva, Elisabete, Luísa Barreiros, Marcela A. Segundo, Sofia a. Costa Lima, and Salette Reis. 2017. "Cellular Interactions of a Lipid-based Nanocarrier Model With Human Keratinocytes: Unravelling Transport Mechanisms." *Acta Biomaterialia* 53 (4): 439–49. https://doi.org/10.1016/j.actbio.2017.01.057.

Spetsieris, Konstantinos, and Kyriacos Zygourakis. 2012. "Single-cell Behavior and Population Heterogeneity: Solving an Inverse Problem to Compute the Intrinsic Physiological State Functions." *Journal of Biotechnology* 158 (3): 80–90. https://doi.org/10.1016/j.jbiotec.2011.08.018.

Spitzer, Matthew H., and Garry P. Nolan. 2016. "Mass Cytometry: Single Cells, Many Features." *Cell* 165 (4): 780–91. https://doi.org/10.1016/j.cell.2016.04.019.

Trajkovic, Katarina, Clarissa Valdez, Daniel Ysselstein, and Dimitri Krainc. 2019. "Fluctuations in Cell Density Alter Protein Markers of Multiple Cellular Compartments, Confounding Experimental Outcomes." *PLoS ONE* 14 (2): e0211727. https://doi.org/10.1371/journal.pone.0211727.

Torres-Cruz, Fred, K. Nerkar Charushila, S. Chobe Santosh, N. Subasree, Abhishek Madduri, and Bhasker Pant. 2023. "A Review on Future Prospects on Magnetic Levitation for Disease Diagnosis." *AIP Conference Proceedings*, (1): 0400091. https://doi.org/10.1063/5.0126243.

Turnbull, Gareth, Jon Clarke, Frédéric Picard, Weidong Zhang, Philip Riches, Bin Li, and Wenmiao Shu. 2020. "3D Biofabrication for Soft Tissue and Cartilage Engineering." *Medical Engineering & Physics* 82 (8): 13–39. https://doi.org/10.1016/j.medengphy.2020.06.003.

Vedula, Sri Ram Krishna, Hiroaki Hirata, Mui Hoon Nai, Agustı´ Brugués, Yusuke Toyama, Xavier Trepat, Chwee Teck Lim, and Benoit Ladoux. 2013. "Epithelial Bridges Maintain Tissue Integrity During Collective Cell Migration." *Nature Materials* 13 (1): 87–96. https://doi.org/10.1038/nmat3814.

Vig, Komal, Atul Chaudhari, Shweta Tripathi, Saurabh Dixit, Rajnish Sahu, Shreekumar Pillai, Vida Dennis, and Shree Singh. 2017. "Advances in Skin Regeneration Using Tissue Engineering." *International Journal of Molecular Sciences* 18 (4): 789. https://doi.org/10.3390/ijms18040789.

Vyas, Krishna S, and Henry C Vasconez. 2014. "Wound Healing: Biologics, Skin Substitutes, Biomembranes and Scaffolds." *Healthcare* 2 (3): 356–400. https://doi.org/10.3390/healthcare2030356.

Wang, Weibin, Jiajia Dai, Yufeng Huang, Xiaomeng Li, Jianmin Yang, Yunquan Zheng, and Xianai Shi. 2023. "Extracellular Matrix Mimicking Dynamic Interpenetrating Network Hydrogel for Skin Tissue Engineering." *Chemical Engineering Journal* 457 (2): 141362. https://doi.org/10.1016/j.cej.2023.141362.

Wang, Xian, Junhui Law, Mengxi Luo, Zheyuan Gong, Jiangfan Yu, Wentian Tang, Zhuoran Zhang, et al. 2020. "Magnetic Measurement and Stimulation of Cellular and Intracellular Structures." *ACS Nano* 14 (4): 3805–21. https://doi.org/10.1021/acsnano.0c00959.

Watt, Fiona M. 2014. "Mammalian Skin Cell Biology: At the Interface Between Laboratory and Clinic." *Science* 346 (6212): 937–40. https://doi.org/10.1126/science.1253734.

Werner, Sabine, Thomas Krieg, and Hans Smola. 2007. "Keratinocyte–Fibroblast Interactions in Wound Healing." *Journal of Investigative Dermatology* 127 (5): 998–1008. https://doi.org/10.1038/sj.jid.5700786.

Wychowaniec, Jacek K., and Dermot F. Brougham. 2022. "Emerging Magnetic Fabrication Technologies Provide Controllable Hierarchically-Structured Biomaterials and Stimulus Response for Biomedical Applications." *Advanced Science* 9 (34): e2202278. https://doi.org/10.1002/advs.202202278.

Wysocki, Annette B. 1999. "Skin Anatomy, Physiology, And Pathophysiology." *Nursing Clinics of North America* 34 (4): 777–97. https://doi.org/10.1016/s0029-6465(22)02423-9.

Yaman, Sena, Muge Anil-Inevi, Engin Ozcivici, and Hüseyin C. Tekin. 2018. "Magnetic Force-Based Microfluidic Techniques for Cellular and Tissue Bioengineering." *Frontiers in Bioengineering and Biotechnology* 6 (12): 192. https://doi.org/10.3389/fbioe.2018.00192.

Yamato, Masafumi, and Tsunehisa Kimura. 2020. "Magnetic Processing of Diamagnetic Materials." *Polymers* 12 (7): 1491. https://doi.org/10.3390/polym12071491.

Yang, Ruey Jen, Hui Hsiung Hou, Yao Nan Wang, and Lung Ming Fu. 2016. "Micro-magnetofluidics in Microfluidic Systems: A Review." *Sensors and Actuators B Chemical* 224 (3): 1–15. https://doi.org/10.1016/j.snb.2015.10.053.

Yasarbas, S. Suheda, Ece Inal, M. Azra Yildirim, Sandrine Dubrac, Jérôme Lamartine, and Gulistan Mese. 2024. "Connexins in Epidermal Health and Diseases: Insights Into Their Mutations, Implications, and Therapeutic Solutions." *Frontiers in Physiology* 15 (5): 1346971. https://doi.org/10.3389/fphys.2024.1346971.

Yu, Justine R., Javier Navarro, James C. Coburn, Bhushan Mahadik, Joseph Molnar, James H. Holmes, Arthur J. Nam, and John P. Fisher. 2019. "Current and Future Perspectives on Skin Tissue Engineering: Key Features of Biomedical Research, Translational Assessment, and Clinical Application." *Advanced Healthcare Materials* 8 (5): e1801471. https://doi.org/10.1002/adhm.201801471.

Zhao, Wujun, Rui Cheng, Joshua R. Miller, and Leidong Mao. 2016. "Label-Free Microfluidic Manipulation of Particles and Cells in Magnetic Liquids." *Advanced Functional Materials* 26 (22): 3916–32. https://doi.org/10.1002/adfm.201504178.

Zheng, Shuo-Lei, Yu-Mei Wang, Chang-Feng Chi, and Bin Wang. 2024. "Chemical Characterization of Honeysuckle Polyphenols and Their Alleviating Function on Ultraviolet B-Damaged HaCaT Cells by Modulating the Nrf2/NF-κB Signaling Pathways." *Antioxidants* 13 (3): 294. https://doi.org/10.3390/antiox13030294.

Zhong, Jiamin, Hao Wang, Ke Yang, Huifeng Wang, Chongwen Duan, Na Ni, Liqin An, et al. 2022. "Reversibly Immortalized Keratinocytes (iKera) Facilitate Re-epithelization and Skin Wound Healing: Potential Applications in Cell-based Skin Tissue Engineering." *Bioactive Materials* 9 (3): 523–40. https://doi.org/10.1016/j.bioactmat.2021.07.022.

Zhu, Chongtao, Jiankun Liu, Bin He, Xiaowen Qu, and Daizhi Peng. 2019. "The Role of Human Immortal Skin Keratinocytes-acellular Dermal Matrix Scaffold in Skin Repair and Regeneration." *Journal of Cellular Biochemistry* 120 (8): 12182–91. https://doi.org/10.1002/jcb.28588.

Zhu, Taotao, Rui Cheng, Yufei Liu, Jian He, and Leidong Mao. 2014. "Combining Positive and Negative Magnetophoreses to Separate Particles of Different Magnetic Properties." *Microfluidics and Nanofluidics* 17 (6): 973–82. https://doi.org/10.1007/s10404-014-1396-